J. Nonlinear Sci. Vol. 4: pp. 253–299 (1994)

Journal of
Nonlinear
Science

Conserving Algorithms for the Dynamics of Hamiltonian Systems on Lie Groups

D. Lewis[1] and J. C. Simo[2]

[1] Board of Mathematics, University of California Santa Cruz, Santa Cruz, CA 95064, USA

[2] Division of Applied Mechanics, Stanford University, Stanford, CA 94305, USA

Received October 7, 1992; revised manuscript accepted for publication August 8, 1993
Communicated by Jerrold Marsden

Summary. Three conservation laws are associated with the dynamics of Hamiltonian systems with symmetry: The total energy, the momentum map associated with the symmetry group, and the symplectic structure are invariant under the flow. Discrete time approximations of Hamiltonian flows typically do not share these properties unless specifically designed to do so. We develop explicit conservation conditions for a general class of algorithms on Lie groups. For the rigid body these conditions lead to a single-step algorithm that exactly preserves the energy, spatial momentum, and symplectic form. For homogeneous nonlinear elasticity, we find algorithms that conserve angular momentum and either the energy or the symplectic form.

Key words. Hamilton's equations, symmetry groups, canonical transformations, rigid bodies, homogeneous elasticity

1. Introduction

The dynamics of an autonomous Hamiltonian system possesses two fundamental conservation properties. The flow preserves the Hamiltonian function (i.e., conserves energy) and defines a canonical transformation that preserves exactly the symplectic two-form. If the Hamiltonian possesses symmetries induced by the symplectic action of a Lie group on the phase space, additional conserved quantities known as momentum maps arise which are exactly preserved by the Hamiltonian flow; see, for example, Arnold [1988] or Abraham and Marsden [1978]. Typical examples of momentum maps are the total linear and total angular momentum. The preceding conservation laws play a fundamental role in the foundations of classical mechanics and often define observables of primary interest in applications of solid, fluid, and celestial mechanics.

Temporal (and spatial) discretizations of the dynamics generated by a Hamiltonian system need not, and in general will not, inherit the conservation laws of the continuum system. Numerical schemes designed to preserve exactly one or several of the underlying conserved quantities for finite step sizes will be referred to as *conserving algorithms*. At least three considerations motivate the construction of this type of numerical scheme: (1) the fundamental physical and mathematical significance of conserved quantities, (2) the belief that conserved quantities often capture key qualitative features of the long-term dynamics, and (3) the enhanced numerical analysis properties of conserving algorithms. For instance, exact energy conservation is often regarded as a strong manifestation of unconditional numerical stability. The use of a priori energy estimates is in fact the essence of the classical energy method of stability analysis; see, for example, Ritchmyer and Morton [1967] and Morton [1977].

This paper investigates two specific classes of conserving schemes for Hamiltonian systems possessing a *truly nonlinear* configuration space with a group structure: *symplectic integrators*, which define a canonical transformation that conserves invariants such as the volume in phase space (Liouville's theorem), and *energy-momentum conserving algorithms*. Symplectic integrators were introduced in the pioneering work of De Vogelare [1956] (unpublished) and have recently received considerable attention; see for example, Channell [1983], Feng Kan [1986], Feng Kan and Qin [1987], Lasagni [1988], Sanz-Serna [1988], Channell and Scovel [1990], and Zhong and Marsden [1990]. For overviews of the exponentially growing literature on the subject, too extensive to be examined here in any detail, the reader is referred to the review articles of Scovel [1991] and Sanz-Serna [1992]. Energy-momentum conserving algorithms have been considered by a number of authors, including Bayliss and Isaacson [1975], Labbude and Greenspan [1976a,b], Marciniak [1984], and Simo and Wong [1991], often in the context of specific applications. General methodologies applicable to any Hamiltonian system with a configuration manifold open in a linear space are described in Simo and Tarnow [1992]; energy-momentum conserving algorithms for general Hamiltonian systems on $SO(2)$ and $SO(3)$ are given in Simo, Tarnow, and Wong [1992].

1.1. Motivation and Scope of the Paper

Within the setting typically adopted in investigations on symplectic integrators, the configuration space Q is assumed to be *linear*, say, finite dimensional for simplicity ($\dim Q = n$), with canonical phase space $P = T^*Q$ ($\dim P = 2n$). Given a general Hamiltonian $H: P \to \mathbb{R}$ the *canonical* evolution equations then take the standard form

$$\dot{z} = \mathcal{J}\nabla H(z) \quad \text{with} \quad z|_{t=0} = z_0, \tag{1.1}$$

where $\mathcal{J}$ denotes the canonical symplectic matrix and the symplectic two-form ω: $TP \times TP \to \mathbb{R}$ is given by

$$\omega(\delta z_1, \delta z_2) = \delta z_1 \cdot \mathcal{J}\delta z_2 \quad \text{with} \quad \mathcal{J} := \begin{pmatrix} \mathbf{0} & \mathbf{1} \\ -\mathbf{1} & \mathbf{0} \end{pmatrix}. \tag{1.2}$$

A number of results are derived within this framework. For instance, the symplectic character of the implicit midpoint rule (Feng Kan [1986]) or the explicit central dif-

ference method (Simo, Tarnow, and Wong [1992]), and the explicit characterization of symplectic members within the classical family of Runge–Kutta methods (Lasagni [1988] and Sanz-Serna [1988]).

The preceding setting, however, does not apply to nonlinear problems of evolution in classical mechanics arising in a number of significant applications. For example, for rigid bodies $Q = SO(3)$ is a finite dimensional compact Lie group, for incompressible homogeneous elastic bodies $Q = SL(3)$ is the group of unimodular matrices, for ideal incompressible fixed boundary fluids $Q = \mathrm{Diff}_{\mathrm{vol}}(\Omega)$ is the infinite dimensional group of volume preserving diffeomorphisms on $\Omega \subset \mathbb{R}^3$, while for three-dimensional incompressible elasticity $Q = \mathrm{Emb}_{\mathrm{vol}}(\Omega, \mathbb{R}^3)$ is the differentiable manifold of volume preserving embeddings from Ω into $\mathbb{R}^3$. The proper mathematical setting of these and many other examples is that of *simple mechanical systems* in the sense of Smale [1970]: the configuration space Q is a differentiable manifold, often (but not always) a Lie group, and the canonical phase is the cotangent bundle $P = T^*Q$. In addition, the Hamiltonian $H: P \to \mathbb{R}$ is invariant relative to the symplectic action of a Lie group G on P with equivariant momentum map $\mathbf{J}: P \to \mathcal{G}^*$, where $\mathcal{G}^*$ is the dual of the Lie algebra.

A key question addressed in this paper is, To what extent can conserving algorithms and algorithm design strategies derived in the restricted setting of Hamiltonian systems on a linear phase space be applied to mechanical systems on general manifolds? This question can be motivated by the following elementary example.

Example. Consider the simple example afforded by the dynamics of a pendulum of mass $m > 0$ in a force field with potential function $V: \mathbb{R}^3 \to \mathbb{R}$. The configuration space for this mechanical system is the unit sphere $Q = S^2$, with canonical phase space the cotangent bundle $P := T^*S^2$. Denoting by $\mathbf{q} \in Q$ the position vector of the point mass m relative to the fixed point, which is taken as the origin of a Cartesian coordinate system, the Hamiltonian function $H: P \to \mathbb{R}$ can be written as

$$H(\mathbf{z}) = K(\pi) + V(\mathbf{q}), \qquad K(\pi) := \frac{1}{2m}\|\pi\|^2, \tag{1.3}$$

where $\pi := m\mathbf{q} \times \dot{\mathbf{q}}$ is the generalized (angular) momenta, and $\mathbf{z} = (\mathbf{q}, \pi)$ denotes a point in the canonical phase space. Obviously P is a four-dimensional manifold which is *not* a vector space. Elementary considerations show that Hamilton's equations of motion can be written in the canonical form (1.1). However, the symplectic matrix $\mathcal{J}(\mathbf{z})$ is *configuration dependent* and given by

$$\mathcal{J}(\mathbf{z}) := \begin{pmatrix} \mathbf{0} & -\hat{\mathbf{q}} \\ -\hat{\mathbf{q}} & \mathbf{0} \end{pmatrix}. \tag{1.4}$$

Here $\hat{\mathbf{q}}$ denotes the skew-symmetric matrix associated with the vector $\mathbf{q}$, defined by the relation $\hat{\mathbf{q}}\mathbf{h} = \mathbf{q} \times \mathbf{h}$ for any vector $\mathbf{h} \in \mathbb{R}^3$. To make matters even simpler, consider a force field with constant direction defined by a unit vector $\gamma \in S^2$, so that $V(\mathbf{q}) := -g(\gamma \cdot \mathbf{q})$ where $g: \mathbb{R} \to \mathbb{R}$ can be interpreted as the intensity of a generally non-constant gravitational field. Under these conditions, the Hamiltonian (1.3) is invariant under rotations about γ and the momentum map $J_\gamma: P \to \mathbb{R}$, defined as

$$J_\gamma(\mathbf{z}) = \pi \cdot \gamma \quad \text{(angular momentum about the axis } \gamma\text{)}, \tag{1.5}$$

is a constant of the motion. The system is completely integrable since the presence of two conserved quantities, H and J_γ, yield a reduced phase space $\widetilde{P}$ isomorphic to the two-dimensional torus.

To illustrate the issues that arise when the phase space is no longer linear, we consider the numerical time-integration of this completely integrable Hamiltonian system by the midpoint rule. The algorithmic counterpart of equation (1.1) is

$$\mathbf{z}_{n+1} - \mathbf{z}_n = \Delta t \mathcal{J}\left(\tfrac{1}{2}(\mathbf{z}_{n+1} + \mathbf{z}_n)\right)\nabla H\left(\tfrac{1}{2}(\mathbf{z}_n + \mathbf{z}_n)\right). \tag{1.6}$$

Note that the Hamiltonian (1.3) and the map $\mathcal{J}$ (1.4) can be extended to $T^*\mathbb{R}^3$; thus (1.6) can be defined even though $\frac{1}{2}(\mathbf{z}_{n+1} + \mathbf{z}_n)$ is typically not an element of T^*P. Assume that the algorithmic initial data $\mathbf{z}_n := (\mathbf{q}_n, \pi_n)$ at time $t = t_n$ is in P, so that $\|\mathbf{q}_n\| = 1$ and $\pi_n \cdot \mathbf{q}_n = 0$. The reader can easily verify the following results (for a detailed analysis of this problem see the review article of Simo and Gonzalez [1993]):

1. The algorithmic approximation $\mathbf{z}_{n+1} = (\mathbf{q}_{n+1}, \pi_{n+1})$ lies in $P = T^*S^2$. Equivalently, algorithm (1.6) exactly preserves the constraints $\|\mathbf{q}_{n+1}\| = 1$ and $\pi_{n+1} \cdot \mathbf{q}_{n+1} = 0$.
2. Algorithm (1.6) is exact momentum preserving, in the sense that $J_\gamma(\mathbf{z}_n) = J_\gamma(\mathbf{z}_n)$. In addition, if the function $g(\cdot)$ is at most quadratic, the algorithm exactly preserves the Hamiltonian in the sense that $H(\mathbf{z}_{n+1}) = H(\mathbf{z}_n)$.
3. When applied to a system with linear phase space, the midpoint rule is symplectic; in fact, it is the lowest order symplectic Runge–Kutta method. Remarkably, however, algorithm (1.6) *is not symplectic.*

The parametrization of P used in the preceding formulation of the problem is *global* and, in many ways, analogous to the optimal parametrization of the rotation group in terms of unit quaternions. Alternatively, one may consider a parametrization of the problem in terms of local charts relative to which the symplectic two-form is constant and given by (1.2). By Darboux's theorem, such a local parametrization is guaranteed to exist. However, the possible advantages of working with a simple expression for the symplectic form are often offset by difficulties introduced by the parametrization. One drawback associated with local charts is the inevitable appearance of singularities. For the problem at hand, spherical coordinates provide a *local* Darboux chart. The singularity arises from the fact that it is not possible to cover the unit sphere with a single two-dimensional chart. It is for this reason that global parametrizations are preferred in applications. For the rotation group, for instance, unit quaternions parameters are almost universally used in attitude dynamics, while the familiar Euler angles are seldom implemented in numerical algorithms. Singularities are a well-known difficulty with local coordinate charts; other, more subtle problems associated with conservation laws also arise. Assume that spherical coordinates are used to parametrize the pendulum. Then

4. The midpoint rule retains its symplectic character and is exact momentum preserving when the dynamics is parametrized in spherical coordinates.

5. Remarkably, however, neither the midpoint rule nor any high-order symplectic Runge–Kutta method conserve energy when the dynamics is formulated in spherical coordinates, even in the simple case $g(\mathbf{q}\cdot\gamma) = \mathbf{q}\cdot\gamma$ corresponding to constant gravity acceleration. The reason is that a trigonometric function cannot be integrated exactly regardless of the accuracy of the numerical method.

The conclusion to be drawn from this elementary example is that conventional conserving algorithms on vector spaces need not, and in general will not, retain their conservative properties when applied to a nonlinear manifold Q. Accordingly, the construction of symplectic schemes has to be undertaken on a case-by-case basis. For the elementary problem at hand, for instance, it can be shown that the algorithm (1.6) becomes symplectic and retains second-order accuracy if the average values $\frac{1}{2}(\mathbf{q}_{n+1} + \mathbf{q}_n)$ on the right-hand side of (1.6) are replaced by the scaled values $\mathbf{q}_{n+(1/2)} := \frac{1}{2}(\mathbf{q}_{n+1} + \mathbf{q}_n)/\|\frac{1}{2}(\mathbf{q}_{n+1} + \mathbf{q}_n)\|$. Observe that this scaling ensures that $\mathbf{q}_{n+1/2}$ lies on S^2. □

The goal of this paper is to address the question raised above when the configuration space Q happens to be a Lie group. We focus on dynamics of Lie groups for two reasons: (1) they appear in a variety of important physical systems and (2) the structure of a Lie group makes it possible to specify geometrically precise algorithms (although the actual implementation of such algorithms may be quite difficult). A key feature of linear configuration manifolds is the freedom to take arbitrary linear combinations of variations, that is, tangent vectors. For a closed nonlinear manifold, this is not directly possible. It is necessary to first translate variations to a common vector space before combining them and then translate the result to the appropriate tangent space. In addition, incremental updates of the configuration require some generalized form of exponentiation. The geometric structure of Lie groups provides a framework within which these operations can be carried out. Right or left translations are used to map the tangent space at an arbitrary element of the group onto the Lie algebra—a linear space—where the algorithm is formulated. The resulting algebra element is then mapped to a group element by means of the group exponential map and appropriately translated. Another context in which such constructions exist is Riemannian manifolds. Such manifolds possess a connection, which specifies the appropriate "parallel translation" of variations from one tangent space to another; the existence of an exponential map is also guaranteed. In general, however, such connections and exponentials are quite complicated and are typically implicitly defined.

1.2. Summary of Results

To further illustrate the difficulties involved in the generalization of conserving schemes on linear spaces to simple mechanical systems, in Section 2 and Section 3 we consider in detail the dynamics on the rotation group. This specific example has a significant interest in its own right. Important applications range from celestial mechanics and robotics to classical rigid body dynamics. Moreover, this algorithm can be used as a building block in the design of symplectic schemes for infinite dimensional dynamical systems involving maps from an open set either on the real line or the plane into the rotation group, such as classical models of nonlinear rods

and shells. We also remark that the proposed one-step method encompasses, as a particular case, the energy-momentum algorithms of Simo and Wong [1991] and the subsequent Lie-Poisson integrator of Austin et al. [1992]. Noteworthy results include the following:

- Derivation of the conditions for the preceding class of algorithms to define a symplectic transformation. In sharp contrast with the geometric setting implicit in (1.1) the symplectic two-form in the classical spatial or body descriptions of rigid body dynamics *does not* take the canonical form given in (1.2).
- Identification of a scheme which, to our knowledge, provides the first numerically tractable one-step exact energy-momentum preserving and symplectic integrator for the rotation group. We remark that neither of the two schemes referred to above are symplectic. The new scheme appears to be optimal in the sense that the algorithmic flow differs from the exact flow only by a time reparamtrization.
- Derivation of explicit error estimates on the lack of symplectic character of the general class of energy-momentum algorithms for the Euler equations. The symplectic character of the new energy-momentum algorithm and the significance of the failure of the symplectic property in the two aforementioned schemes is assessed in numerical simulations.

Remark. Discrete-time versions of the generalized rigid body dynamics on $O(n)$ that preserve the energy and symplectic form have been found by Moser and Veselov [1991]. These multistep discrete dynamical systems do not conserve momentum. Specifically, the image of the computed configurations and body momenta under the spatial momentum map is not constant. However, there are one-to-one maps of the trajectories into the spatial momentum level set.

In Section 4 we generalize the preceding results to a general Hamiltonian that includes an additional potential for (nonzero) external loading. A model problem to keep in mind is the dynamics of a heavy rigid body in a gravitational field, a nonintegrable system in the general case.

- Starting from a general class of momentum-conserving algorithms, an explicit condition for exact energy conservation is derived. For the general heavy rigid body, enforcement of this condition yields a concrete energy- and momentum-conserving algorithm generalizing the midpoint rule which is not symplectic, but *is* unconditionally stable and second-order accurate.
- The symplectic conditions for the momentum-conserving generalized midpoint algorithms are shown to imply conservation of the kinetic energy, not the total energy. Thus enforcement of the symplectic condition for these algorithms yields schemes which are not consistent with the governing equations. Although symplectic algorithms could, in principle, be identified within a larger class using the general conditions given in Section 5, the complexity of these conditions makes this task highly nontrivial even for the rotation group.

In Section 5 we consider the generalization of the results presented in the preceding sections to the Hamiltonian dynamics on a general closed Lie group G governed by the generalized Euler equations, as described in the fundamental work of Arnold [1966]. Assuming that a map from the Lie algebra to the group is available (for instance, the exponential map) the following results are shown to hold:

- The structure of the energy- and momentum-conserving algorithms for the rotation group carries over to the case of a general Lie group. The result for the Euler equations is the algorithmic counterpart of the analogy between the classical and generalized Euler equations set forth in Arnold [1966].
- Explicit conditions for a general class of momentum-conserving algorithms to be symplectic are derived. Simplifications of these conditions are also described for the case in which the group G is abelian.

From a practical standpoint, the key obstacle in the implementation of conserving algorithms for the Euler equations is the explicit characterization of the exponential map. (For systems with nontrivial potential, specification of symplectic algorithms appears to be difficult even when a map from the algebra to the group can be explicitly identified.) A closed-form expression is generally not known—exceptions are the rotation group, the symplectic groups, and linear groups. In Section 6, this difficulty is circumvented in the case where the configuration manifold is open in a larger linear space. For instance, for homogeneous compressible elasticity $Q = GL(3)$ is open $L(3)$. Additional examples of interest in applications include the compressible Euler equations and compressible nonlinear elasticity. The key idea here is to replace the (multiplicative) configuration update by the simpler additive update on the larger linear space. This technique is widely used in finite element treatments of a number of problems including nonlinear elasticity (see, e.g., Simo and Taylor [1991] and references therein). Adopting this strategy, we show that

- Energy-momentum algorithms can be developed which conserve the true momentum map and the true Hamiltonian function of a *given* Hamiltonian system. An explicit example for the case of homogeneous elasticity is given following the methodology recently proposed in Simo and Tarnow [1992].
- Algorithms such as the implicit midpoint rule and the central difference method retain their symplectic character since, in the canonical setting, the symplectic two-forms in the phase space and the larger linear space coincide.

The performance of these two classes of algorithms is illustrated by phase portraits of sample numerical simulations.

2. The Dynamics on the Rotation Group

Below we describe our general strategy in the formulation of algorithms for Hamiltonian systems on Lie groups designed to inherit exactly conservation of the momentum map, conservation of energy, and/or the symplectic character of the flow. The construction proceeds in four steps, which are summarized below in the specific setting of the rotation group:

Step 1. Regard the rotation group $SO(3)$ as embedded into a larger group, the linear group $L(3) \supset SO(3)$. Then construct a four-parameter family of exact momentum-preserving schemes by time-stepping in $L(3)$.

Step 2. Restrict the four-parameter family constructed above by enforcing the constraint that the algorithmic flow lies in $SO(3)$. This constraint eliminates one parameter leading to a three-parameter family of exact momentum-conserving schemes in $SO(3)$.

Step 3. Restrict further the three-parameter family of momentum-conserving schemes constructed in Step 2 by enforcing exact energy conservation. Enforcement of this constraint is shown to yield a one-parameter family of exact energy- and momentum-conserving schemes, where the free parameter is in fact an arbitrary functional.

Step 4. Remarkably, for the unreduced Euler equations on $T^*SO(3)$ it is possible to specify the free function in the one-parameter family of exact momentum- and energy-preserving schemes so as to exactly preserve the symplectic structure in $SO(3) \times \mathbb{R}^3 \approx T^*SO(3)$.

A few remarks should be made concerning the general applicability of this strategy. The developments in the subsequent sections suggest that the simultaneous completion of steps 3 and 4 above is not possible for a general Lie group G or even a general Hamiltonian system on the rotation group. This difficulty could be related to the fact, first pointed out in Zhong and Marsden [1990], that symplectic schemes for nonintegrable systems which exactly conserve energy must differ from the exact flow only by a time-reparametrization. Integrability considerations, however, place no restrictions on the design of algorithms that simultaneously conserve the Hamiltonian and the momentum map. The integrability property of the Euler equations on the rotation group plays no explicit role in our analysis.

It should be emphasized that the result of Zhong and Marsden quoted above applies *only* to nonintegrable systems and provides no information regarding the existence or absence of completely conserving algorithms for *integrable* systems. In spite of this negative result, the symplectic conditions derived in this paper can be exploited in the design of *approximately* symplectic schemes. For instance, within a given family of energy- and momentum-conserving algorithms one could identify the member which most nearly preserves the symplectic form when modeling nonintegrable systems. For the rotation group, the optimal member identified below turns out to be exactly symplectic.

2.1. Summary of Basic Results on the Rotation Group

We summarize some elementary properties of the rotation group needed for our subsequent developments. Further details can be found in a number of standard textbooks which range from classical treatments, as in Whittaker [1932] or Goldstein [1982], to accounts with a distinctive geometric flavor, as in Coquete-Bruhat and De Witt-Morette [1982], Abraham and Marsden [1978], or Arnold [1988].

2.1.1. Basic Definitions. The rotation group $SO(3)$ is the compact subgroup of the general linear group $GL(3, \mathbb{R})$ consisting of proper orthogonal matrices. Its Lie algebra $so(3)$ is the linear space of skew-symmetric matrices, with Lie bracket $[\cdot, \cdot]$ the ordinary matrix commutator. $\{so(3), [\cdot, \cdot]\}$ is identified with $\{\mathbb{R}^3, \times\}$ via the standard Lie algebra isomorphism $\hat{}: \mathbb{R}^3 \to so(3)$ defined as

$$\hat{\Theta}\mathbf{h} = \Theta \times \mathbf{h} \quad \text{for all } \mathbf{h} \in \mathbb{R}^3, \quad \text{with} \quad [\hat{\Theta}_1, \hat{\Theta}_2] = \widehat{\Theta_1 \times \Theta_2}. \tag{2.1}$$

The dual space to the Lie algebra $so(3)$, denoted by $so(3)^*$, is also identified with $\mathbb{R}^3$ using the Euclidean dot product as duality pairing.

The tangent space $T_\Lambda SO(3)$ at any $\Lambda \in SO(3)$ is obtained via either left or right translations of the Lie algebra, leading to the body or spatial representations. Throughout this paper we shall use these two standard descriptions and, with a slight abuse of notation, write

$$T_\Lambda SO(3) = \{\theta_\Lambda = \hat{\theta}\Lambda = \Lambda\hat{\Theta} : \text{ with } \theta = \Lambda\Theta \in \mathbb{R}^3\}. \tag{2.2}$$

In the context of mechanics, θ and Θ are interpreted as spatial and body (virtual) angular velocities, respectively. In actual computations it proves convenient to use the identification $T_\Lambda SO(3) \approx \mathbb{R}^3 \times SO(3)$ (or $SO(3) \times \mathbb{R}^3$) defined by the mapping $(\theta, \Lambda) \mapsto \theta_\Lambda$ (or $(\Lambda, \Theta) \mapsto \theta_\Lambda$). In a similar fashion, the body (or spatial) identification of the phase space $P := T^*SO(3) \approx \mathbb{R}^3 \times SO(3)$ (or $SO(3) \times \mathbb{R}^3$) is defined via the mapping $(\pi, \Lambda) \mapsto \pi_\Lambda$ (or $(\Lambda, \Pi) \mapsto \pi_\Lambda$).

2.1.2. Mappings from the Lie Algebra to the Group. The update of the configuration in the class of conserving algorithms on Lie groups described below relies crucially on the use of a map from the Lie algebra to the group. The natural choice is the exponential mapping $\exp[\cdot]$, defined for a matrix group via the standard infinite series; see for example, Curtis [1984]. A remarkable fact specific to the rotation group is that the exponential map $\exp : \mathbb{R}^3 \to SO(3)$ admits a closed-form representation given by the classical formula

$$\exp[\Theta] = \cos(|\Theta|)\, 1 + \frac{\sin(|\Theta|)}{|\Theta|}\hat{\Theta} + \frac{1 - \cos(|\Theta|)}{|\Theta|^2}\Theta \otimes \Theta, \tag{2.3}$$

which goes back to Euler and Rodrigues (see Whittaker [1932]). Alternatively, the preceding formula can be recast in the equivalent form

$$\exp[\Theta] = 1 + \frac{2}{1 + |\bar{\Theta}|^2}\left(\hat{\bar{\Theta}} + \hat{\bar{\Theta}}^2\right), \quad \text{where} \quad \bar{\Theta} := \frac{1}{2}\frac{\tan\left(\frac{1}{2}|\Theta|\right)}{\frac{1}{2}|\Theta|}\Theta \tag{2.4}$$

is often referred to as the *pseudo-vector* in the attitude dynamics literature. The closed-form formulas (2.3) and (2.4) are key results exploited in the formulation of attitude dynamic and control algorithms.

For the rotation group, the Cayley transform $\text{cay} : \mathbb{R} \to SO(3)$ defined by the formula

$$\text{cay}[\Theta] := \left(1 + \tfrac{1}{2}\hat{\Theta}\right)\left(1 - \tfrac{1}{2}\hat{\Theta}\right)^{-1} \tag{2.5}$$

also defines a mapping from the Lie algebra $\mathbb{R}^3$ onto the group $SO(3)$. This property holds for the symplectic group but, unfortunately, is not true for a general Lie group. Furthermore, in contrast with the exponential map, the Cayley transform is not singularity-free. Interestingly, for the rotation group the inversion arising in the definition of the Cayley transform can also be computed explicitly using the Neumann series, yielding

$$\operatorname{cay}[\Theta] = 1 + \left(\frac{2}{1 + \left(\frac{1}{2}|\bar{\Theta}|\right)^2} \left(\tfrac{1}{2}\widehat{\Theta}\right) + \left(\tfrac{1}{2}\widehat{\Theta}\right)^2 \right). \tag{2.6}$$

By comparing this expression with the formula for the exponential map in terms of the pseudo-vector, one concludes that

$$\exp \Theta = \operatorname{cay}[\kappa(\Theta)\Theta], \quad \text{where} \quad \kappa(\Theta) = \frac{\tan\left(\frac{1}{2}|\Theta|\right)}{\frac{1}{2}|\Theta|}. \tag{2.7}$$

This property does not appear to be well-known and plays an important role in the formulation of symplectic schemes for the rotation group, discussed below. We remark that the exponential map provides the *exact* rotational update of arbitrary vectors in $\mathbb{R}^3$, a property which motivates its widespread use in attitude dynamic. This appealing feature is not shared by the Cayley transform.

2.1.3. The Symplectic Two-Form. As was pointed out above, the spatial (or body) identification $P = T^*SO(3) \approx \mathbb{R}^3 \times SO(3)$ of the phase space provides a convenient parametrization for actual calculations. If we identify an element $\delta\pi_\Lambda$ of the tangent space $T_{\pi_\Lambda}P$ with the pair $(\delta\theta, \delta\pi) \in \mathbb{R}^3 \times \mathbb{R}^3$ satisfying

$$\delta\pi_\Lambda = \widehat{\delta\bar{\pi}}\Lambda + \widehat{\bar{\pi}\delta\bar{\theta}}\Lambda, \tag{2.8}$$

then the spatial expression for symplectic form is

$$\begin{aligned} \omega(\delta\pi_\Lambda, \delta\bar{\pi}_\Lambda) &= \delta\bar{\pi} \cdot \delta\theta - \delta\pi \cdot \delta\bar{\theta} - \pi \cdot \left(\delta\theta \times \delta\bar{\theta}\right) \\ &= \begin{pmatrix} \delta\theta^T & \delta\pi^T \end{pmatrix} \begin{pmatrix} \hat{\pi} & \mathbf{1} \\ -\mathbf{1} & \mathbf{O} \end{pmatrix} \begin{pmatrix} \delta\bar{\theta} \\ \delta\bar{\pi} \end{pmatrix}. \end{aligned} \tag{2.9}$$

Observe that the matrix appearing in this bilinear form is *not* the standard canonical symplectic matrix. The preceding result, which will be used in the analysis of the symplectic character of the algorithms described below, is a special case of the general formula for the right-trivialized representation of the symplectic two-form, which is derived in Section 5.1.

2.1.4. Dynamics on $SO(3)$: Euler Equations and Momentum Maps. Since the orientation of a rigid body is completely specified by the attitude matrix Λ, which defines the orientation of the body frame relative to the inertia frame, the configuration manifold of the rigid body is the group $SO(3)$ and the canonical phase space is $P = T^*SO(3)$. The spatial and body angular velocities, respectively denoted by ω and Ω, then satisfy the relation

$$\dot{\Lambda} = \hat{\omega}\Lambda = \Lambda\hat{\Omega}, \quad \text{so that} \quad \omega = \Lambda\Omega. \tag{2.10}$$

The body angular momentum, denoted by Π, is related to the body velocity via the standard (Legendre) transformation $\Pi = \boldsymbol{J}\boldsymbol{\Omega}$, where $\boldsymbol{J}$ is the *inertia tensor in body coordinates* relative to the center of mass. The spatial angular momentum, denoted by π, is related to the body angular momentum via the relation $\pi = \Lambda^{-T}\Pi = \Lambda\Pi$.

In the presence of zero resultant forces and moments, and relative to an inertial frame attached at the center of mass, the Hamiltonian function $H: P \to \mathbb{R}$ for the rigid body is the total kinetic energy given by

$$H = \tfrac{1}{2}\Pi \cdot \boldsymbol{J}^{-1}\Pi = \tfrac{1}{2}\pi \cdot \left[\Lambda \boldsymbol{J} \Lambda^{T}\right]^{-1} \pi. \tag{2.11}$$

These two equivalent expressions correspond to the body and spatial descriptions of rigid-body dynamics.

With the preceding conventions, the body representation of the (unreduced) form of the classical *Euler equations* governing the dynamics of a rigid body is given by

$$\left.\begin{aligned} \dot{\Lambda} &= \Lambda\hat{\Omega} \\ \dot{\Pi} &= \Pi \times \Omega \end{aligned}\right\}, \quad \text{with} \quad \Pi = \boldsymbol{J}\boldsymbol{\Omega}, \tag{2.12}$$

which includes the evolution equation for the attitude matrix in (2.10). Observe that the second equation is equivalent to the statement that $\dot{\pi} = \mathbf{0}$, a property easily verified by time differentiation of the relation $\pi = \Lambda\Pi$. The equations (2.12) are Hamiltonian with Hamiltonian function H defined by (2.11). Since the system is autonomous, the dynamics exactly conserves energy in the sense that $\dot{H} = 0$.

Inspection of (2.11) reveals that the Hamiltonian is invariant under the left action of $SO(3)$, in the sense that $H(Q\Pi, Q\Lambda) = H(\Pi, \Lambda)$ for any $Q \in SO(3)$. By the Hamiltonian version of Noether's theorem, associated with this invariance property there is an additional conserved quantity, the *momentum map* $\boldsymbol{\Phi} : P \to \mathbb{R}^3$, given by

$$\Phi(\Pi, \Lambda) := \Lambda\Pi \equiv \pi. \tag{2.13}$$

As pointed out above, it follows from the second Euler equation (2.12_2) that $\dot{\boldsymbol{\Phi}} = \mathbf{0}$. Using the preceding four conservation laws, the six-dimensional Euler equations, (2.12) are reduced to two independent equations; that is, a *completely integrable system*. This is the classical reduction process that describes the dynamics in terms of action-angle variables on the two-torus; see, for example, Arnold [1988].

2.2. Exact Energy and Momentum Conserving Schemes

We describe a constructive procedure, outlined above within the specific context of rigid-body dynamics, for the systematic design of time-stepping algorithms that inherit exactly the conservation laws of momentum and energy summarized in the preceding subsection.

Step 1. Regard $SO(3)$ as a submanifold of the linear Lie group $L(3)$ and compute the change in the momentum map as follows:

$$\begin{aligned}\mathbf{\Phi}_{n+1} - \mathbf{\Phi}_n &= \Lambda_{n+1}\Pi_{n+1} - \Lambda_n\Pi_n \\ &= \Lambda_{n+1}(\Pi_{n+1} - \Pi_n) + (\Lambda_{n+1} - \Lambda_n)\Pi_n. \end{aligned} \tag{2.14}$$

Now define

$$\left.\begin{aligned}\Lambda_{n+\alpha} &:= \alpha\Lambda_{n+1} + (1-\alpha)\Lambda_n \\ \Pi_{n+\alpha} &:= \alpha\Pi_{n+1} + (1-\alpha)\Pi_n\end{aligned}\right\}, \quad \alpha \in [0, 1]. \tag{2.15}$$

A direct computation then shows that

$$\mathbf{\Phi}_{n+1} - \mathbf{\Phi}_n = \Lambda_{n+\alpha}(\Pi_{n+1} - \Pi_n) + (\Lambda_{n+1} - \Lambda_n)\Pi_{n+(1-\alpha)}. \tag{2.16}$$

Motivated by (2.16) we consider the following four-parameter family of algorithms

$$\left.\begin{aligned}\Lambda_{n+1} - \Lambda_n &= \Lambda_{n+\alpha}\widehat{\Theta} \\ \Pi_{n+1} - \Pi_n &= \Pi_{n+(1-\alpha)} \times \Theta\end{aligned}\right\}, \quad \alpha \in [0, 1], \tag{2.17}$$

where the vector $\Theta \in \mathbb{R}^3$ is at this stage completely arbitrary. The difference in momentum maps predicted by this scheme is then computed to be

$$\mathbf{\Phi}_{n+1} - \mathbf{\Phi}_n = -\Lambda_{n+\alpha}\widehat{\Theta}\Pi_{n+(1-\alpha)} + \Lambda_{n+\alpha}\widehat{\Theta}\Pi_{n+(1-\alpha)} = 0 \tag{2.18}$$

for all $\alpha \in [0, 1]$ and all $\Theta \in \mathbb{R}^3$. Consequently, we have

Result 1. *The algorithm (2.17) exactly preserves total angular momentum for any* $\Theta \in \mathbb{R}^3$ *and any* $\alpha \in [0, 1]$.

Note that the scheme (2.17) need not be consistent and, nevertheless, exact momentum conservation is achieved. Furthermore, a standard calculation using Taylor series expansions shows that consistency of the scheme (2.17) with the continuum dynamics is ensured provided that $\Theta = (\Delta t/2)\mathbf{J}^{-1}(\Pi_{n+1} + \Pi_n) + \mathbb{O}(\Delta t^2)$, regardless of the value $\alpha \in [0, 1]$.

Step 2. Scheme (2.17) *does not* guarantee that $\Lambda_{n+1} \in SO(3)$ for given $\Lambda_n \in SO(3)$. We show that enforcement of the condition that Λ_{n+1} be in $SO(3)$ restricts $\alpha \in [0, 1]$ to $\alpha = \frac{1}{2}$. In fact, solving for $(\Lambda_{n+1}, \Pi_{n+1}) \in \mathbf{L}(3) \times \mathbb{R}^3$ in terms of (Λ_n, Π_n) gives

$$\left.\begin{aligned}\Lambda_{n+1} - \Lambda_n\mathbf{T}_\alpha(\Theta) &= \mathbf{0} \\ \mathbf{T}_\alpha(\Theta)\Pi_{n+1} - \Pi_n &= \mathbf{0}\end{aligned}\right\}, \tag{2.19}$$

where

$$\mathbf{T}_\alpha(\Theta) := \left(\mathbf{1} - \alpha\widehat{\Theta}\right)^{-1}\left(\mathbf{1} + (1-\alpha)\widehat{\Theta}\right). \tag{2.20}$$

The equivalent expression (2.19) shows that Λ_{n+1} will be in $SO(3)$ for given Λ_n in $SO(3)$ if $\widetilde{\mathbf{T}}_\alpha(\Theta)$ defines a map from $\mathbb{R}^3$ ($so(3)$) to $SO(3)$. To see when this is the case, we use the standard Neumann series, along with standard properties of skew-symmetric matrices, to compute explicitly

$$\mathbf{T}_\alpha(\Theta) = \mathbf{1} + \frac{1}{1+\alpha^2|\Theta|^2}\left(\widehat{\Theta} + (1-\alpha)\widehat{\Theta}^2\right). \tag{2.21}$$

An easy computation then gives

$$\mathbf{T}_\alpha(\Theta)\mathbf{T}_\alpha(\Theta)^T = \mathbf{1} + \nu\widehat{\Theta}^2, \quad \text{where} \quad \nu := \frac{(1-2\alpha)\left(1-(1-\alpha)^2|\Theta|^2\right)}{\left(1+\alpha^2|\Theta|^2\right)^2}. \tag{2.22}$$

Since $\nu = 0$ for $\alpha = \frac{1}{2}$, leading to $\mathbf{T}_{\frac{1}{2}}(\Theta)\mathbf{T}_{\frac{1}{2}}(\Theta)^T = \mathbf{1}$, we have

Result 2. *The algorithm (2.19) yields $\Lambda_{n+1} \in SO(3)$ for given $\Lambda_n \in SO(3)$ provided that $\alpha = \frac{1}{2}$. In fact, for $\alpha = \frac{1}{2}$ the transformation*

$$\mathbf{T}_\alpha(\Theta)\big|_{\alpha=\frac{1}{2}} = \mathrm{cay}[\Theta] \tag{2.23}$$

mapping $\mathbb{R}^3$ into $SO(3)$ is the Cayley transform defined by (2.5) or, equivalently, by (2.6).

A straightforward manipulation of relations (2.19) yields the following equivalent form of the algorithm for $\alpha = \frac{1}{2}$:

$$\left.\begin{aligned} \Lambda_{n+1} &= \Lambda_n \mathrm{cay}[\Theta] \\ \Pi_{n+1} &= \mathrm{cay}[-\Theta]\Pi_n \end{aligned}\right\}. \tag{2.24}$$

The algorithm (2.24) (or (2.19) defines an exact momentum-preserving scheme whose associated flow lies exactly in $T^*SO(3) \approx SO(3) \times \mathbb{R}^3$ for *any* $\Theta \in \mathbb{R}^3$ and $\alpha = \frac{1}{2}$. Observe that the number of "free parameters" in this exact momentum-conserving scheme equals the dimension, $n_{\mathrm{dim}} = 3$, of the quotient space $T^*SO(3)/SO(3)$ obtained via reduction of the problem by enforcing conservation of momentum.

Step 3. Our aim is to constrain further the scheme (2.19) with $\alpha = \frac{1}{2}$ (i.e., the scheme (2.24)) by enforcing exact conservation of energy. Define

$$\Omega_{n+(1/2)} := \tfrac{1}{2}\boldsymbol{J}^{-1}(\Pi_n + \Pi_{n+1}), \tag{2.25}$$

that is, the angular velocity in body coordinates associated with a midpoint approximation ($\alpha = \frac{1}{2}$). By definition we have

$$\begin{aligned} H_{n+1} - H_n &:= \tfrac{1}{2}\Pi_{n+1}\cdot\boldsymbol{J}^{-1}(\Pi_{n+1} - \tfrac{1}{2}\Pi_n\cdot\boldsymbol{J}^{-1}\Pi_n \\ &= \tfrac{1}{2}(\Pi_{n+1} - \Pi_n)\cdot\boldsymbol{J}^{-1}(\Pi_{n+1} + \Pi_n) \\ &= (\Pi_{n+1} - \Pi_n)\cdot\Omega_{n+(1/2)}. \end{aligned} \tag{2.26}$$

Inserting the algorithmic approximation $(2.17)_2$ into this expression gives

$$H_{n+1} - H_n = \Pi_{n+(1/2)} \times \Theta \cdot \Omega_{n+a(1/2)}. \tag{2.27}$$

Clearly, $H_{n+1} = H_n$ if Θ is parallel to $\Omega_{n+(1/2)}$. Consequently

Result 3. *For the exact momentum-conserving scheme (2.17) with* $\alpha = \frac{1}{2}$, *exact preservation of energy is achieved provided that*

$$\Theta = \kappa(\bar{\Theta})\bar{\Theta} \quad \text{with} \quad \bar{\Theta} := \Delta t \Omega_{n+(1/2)} = \frac{\Delta t}{2} J^{-1}(\Pi_n + \Pi_{n+1}), \tag{2.28}$$

where $\kappa: \mathbb{R}^3 \to \mathbb{R}$ *is a completely arbitrary function.*

A standard argument using Taylor series expansions shows that consistency of the scheme is achieved provided that $\kappa = 1 + \mathbb{O}(|\bar{\Theta}|^2)$. Setting $\kappa \equiv 1$ gives a scheme proposed by Austin, Krishnaprasad, and Wan [1992] within the competely different framework of almost Lie–Poisson integrators.

It follows that exact momentum and energy conservation, plus the condition that $\Lambda_{n+1} \in SO(3)$ for given $\Lambda_n \in SO(3)$, defines the scheme (2.17) up to an arbitrary (scaling) function $\kappa(\bar{\Theta})$. Aside from the choice $\kappa \equiv 1$ alluded to above, other options are possible. In particular, in view of property (2.7) it follows that $\exp[\bar{\Theta}] = \text{cay}[\kappa(\bar{\Theta})\bar{\Theta}]$ is an alternative expression for the exponential map in the rotation group when κ is defined as $\kappa(\bar{\Theta}) = \tan\left(\frac{1}{2}|\bar{\Theta}|\right)/\left(\frac{1}{2}|\bar{\Theta}|\right)$. Motivated by this observation, in the energy-momentum scheme proposed in Simo and Wong [1990] the function κ in definition (2.28) is set to

$$\kappa(\bar{\Theta}) = \frac{\tan\left(\frac{1}{2}|\bar{\Theta}|\right)}{\frac{1}{2}|\bar{\Theta}|}, \tag{2.29}$$

which leads to an update of the attitude matrix in terms of the exponential map.

3. A Symplectic Energy- and Momentum-Conserving Algorithm on $SO(3)$

A map taking z_n to z_{n+1} with linearization $\delta z_{n+1} = L_n \delta z_n$ is said to be symplectic if

$$L_n^T \omega(z_{n+1}) L_n = \omega(z_n) \tag{3.1}$$

for all z_n. Since the function κ introduced in Section 2 is arbitrary, we may search for a specific choice for κ which renders the scheme symplectic, thus completing step 4 in the design of momentum-energy-symplectic schemes. It is shown below that such a κ does in fact exist and is given by a fairly simple closed-form expression.

3.1. Symplectic Condition for General Schemes on SO(3)

Our first objective is the derivation of the condition on the algorithm which ensures preservation of the symplectic two-form. Recall that spatial representation of the symplectic form is a function of the spatial momenta alone and hence is constant if the spatial momenta are conserved. To simplify the necessary calculations, we shall rewrite the momentum equation in (2.24) in terms of the spatial momenta and derive the symplecticity conditions by working with the Poisson matrix, which is the inverse of the matrix representation of the symplectic two-form, rather than the symplectic

form itself. Provided that L_n is invertible (for the algorithm (2.24) this is true for "reasonable" values of Θ), condition (3.1) can be equivalently expressed as

$$L_n \omega(z_n)^{-1} L_n^T = \omega(z_{n+1})^{-1}. \tag{3.2}$$

The relationships $\pi_n = \Lambda_n \Pi_n$ and $\pi_{n+1} = \Lambda_{n+1} \Pi_{n+1}$ between the spatial and body momenta at times t_n and t_{n+1} imply that the spatial representation of the general class of algorithms (2.24) takes the form

$$\left.\begin{aligned} \Lambda_{n+1} &= \Lambda_n \mathbf{T}(\bar{\Theta}) \\ \pi_{n+1} &= \pi_n \\ \bar{\Theta} = \Delta t \Omega_{n+(1/2)} &= \frac{\Delta t}{2} \boldsymbol{J}^{-1} \left(\Lambda_{n+1}^T \pi_{n+1} + \Lambda_n^T \pi_n \right) \end{aligned}\right\}, \tag{3.3}$$

where $\mathbf{T}$: $\mathbb{R}^3 \to SO(3)$ is an arbitrary map from the Lie algebra $so(3)$, identified with $\mathbb{R}^3$ in the usual manner, to the Lie group $SO(3)$. In particular, for the specific choice $\mathbf{T} = \text{cay}[\Theta]$, where $\Theta = \kappa \bar{\Theta}$ with $\bar{\Theta} = \Delta t \Omega_{n+(1/2)}$, one recovers the exact energy-momentum-preserving algorithm (2.24) We note that substituting (3.3_1) and (3.3_2) into (3.3_3) yields the equation

$$\bar{\Theta} = \frac{\Delta t}{2} \boldsymbol{J}^{-1} \left(1 + \mathbf{T}(\bar{\Theta}) \right)^T \Pi_n. \tag{3.4}$$

Given (Λ_n, π_n), the updated attitude matrix Λ_{n+1} is determined by finding a fixed point $\bar{\Theta}$ of the map $\Theta \to (\Delta t/2) \boldsymbol{J}^{-1} (\mathbf{1} + \mathbf{T}(\Theta))^T \Pi_n$ and substituting $\bar{\Theta}$ into (3.3_1). The momentum update (3.3_2) is trivial. The following result is proved below:

Result 4. *The general class of algorithms (3.3) is symplectic provided that the following condition holds:*

$$\frac{4}{\Delta t} \text{ skew } (\mathbf{T}(\bar{\Theta}) + \mathbf{1}) \boldsymbol{H}(\bar{\Theta})^{-T} \boldsymbol{J} = \bar{\Pi}_n - \bar{\Pi}_{n+1}. \tag{3.5}$$

where $\Pi_n = \Lambda_n^T \pi_n$ *and* $\Pi_{n+1} = \Lambda_{n+1}^T \pi_{n+1}$ *and the* 3×3 *matrix* $\boldsymbol{H}(\bar{\Theta})$ *is defined by the relation* $DT(\boldsymbol{\Theta}) \cdot \delta\bar{\Theta} = \mathbf{T}(\Theta) \widehat{[\boldsymbol{H}(\bar{\Theta}) \delta\bar{\Theta}]}$.

Condition (3.5) is proved by directly checking the definition of symplectic map via the following calculation. Using the definition of $\boldsymbol{H}$ and the chain rule, the linearized algorithmic equations become

$$\left.\begin{aligned} \widehat{\delta\theta}_{n+1} \Lambda_{n+1} &= \widehat{\delta\theta}_n \Lambda_{n+1} + \Lambda_n \widehat{\mathbf{T}(\bar{\Theta}) \boldsymbol{H}_n \delta\bar{\Theta}}, \\ \delta\pi_{n+1} &= \delta\pi_n, \end{aligned}\right. \tag{3.6}$$

where $\boldsymbol{H}_n := \boldsymbol{H}(\bar{\Theta})$ for $\bar{\Theta}$ given by (3.3) and $\delta\bar{\Theta}$ is given by

$$\delta\bar{\Theta} = \frac{\Delta t}{2} \boldsymbol{J}^{-1} \left(\Lambda_{n+1}^T (\delta\pi_{n+1} + \pi_{n+1} \times \delta\theta_{n+1}) + \Lambda_n^T (\delta\pi_n + \pi_n \times \delta\theta_n) \right). \tag{3.7}$$

Noting that the first matrix equation (3.6_1) is equivalent to the vector equation $\delta\theta_{n+1} = \delta\theta_n + \Lambda_{n+1} \boldsymbol{H}_n \delta\bar{\Theta}$, we write the system (3.6) in matrix form as

$$\begin{pmatrix} \mathbf{1} + B_{n+1}\hat{\pi} & B_{n+1} \\ \mathbf{0} & \mathbf{1} \end{pmatrix} \begin{pmatrix} \delta\theta_{n+1} \\ \delta\pi_{n+1} \end{pmatrix} = \begin{pmatrix} \mathbf{1} + B_n\hat{\pi} & B_n \\ \mathbf{0} & 1 \end{pmatrix} \begin{pmatrix} \delta\theta_n \\ \delta\pi_n \end{pmatrix}, \tag{3.8}$$

where we have used the abbreviations

$$\left.\begin{aligned} B_n &= M\Lambda_n^T \\ B_{n+1} &= -M\Lambda_{n+1}^T \\ M &= \frac{\Delta t}{2}\Lambda_{n+1}\boldsymbol{H}_n\boldsymbol{J}^{-1} \end{aligned}\right\}. \tag{3.9}$$

To check whether the algorithmic flow is symplectic we use the identity

$$\begin{pmatrix} U & V \\ \mathbf{0} & \mathbf{1} \end{pmatrix} \begin{pmatrix} \mathbf{0} & -\mathbf{1} \\ \mathbf{1} & \hat{\pi} \end{pmatrix} \begin{pmatrix} U & V \\ \mathbf{0} & \mathbf{1} \end{pmatrix}^T = \begin{pmatrix} 2\,\mathrm{skew}[VU^T] + V\hat{\pi}V^T & V\hat{\pi} - U \\ \hat{\pi}V^T + U^T & \hat{\pi} \end{pmatrix} \tag{3.10}$$

for $U, V \in L(3)$. It follows that the symplectic condition

$$\begin{aligned} &\begin{pmatrix} \mathbf{1} + B_{n+1}\hat{\pi} & B_{n+1} \\ \mathbf{0} & \mathbf{1} \end{pmatrix} \begin{pmatrix} \mathbf{0} & -\mathbf{1} \\ \mathbf{1} & \hat{\pi} \end{pmatrix} \begin{pmatrix} \mathbf{1} + B_{n+1}\hat{\pi} & B_{n+1} \\ \mathbf{0} & \mathbf{1} \end{pmatrix}^T \\ &\quad = \begin{pmatrix} \mathbf{1} + B_n\hat{\pi} & B_n \\ \mathbf{0} & \mathbf{1} \end{pmatrix} \begin{pmatrix} \mathbf{0} & -\mathbf{1} \\ \mathbf{1} & \hat{\pi} \end{pmatrix} \begin{pmatrix} \mathbf{1} + B_n\hat{\pi} & B_n \\ \mathbf{0} & \mathbf{1} \end{pmatrix}^T \end{aligned} \tag{3.11}$$

holds if and only if

$$B_{n+1}\left(2\,\mathrm{skew}\left[B_{n+1}^{-T}\right] - \hat{\pi}\right)B_{n+1}^T = B_n\left(2\,\mathrm{skew}\left[B_n^{-T}\right] - \hat{\pi}\right)B_n^T. \tag{3.12}$$

Equation (3.12) can be further simplified by using the regroupings

$$B_{n+1}\left(2\,\mathrm{skew}\left[B_{n+1}^{-T}\right] - \hat{\pi}\right)B_{n+1}^T = -M\left(\frac{4}{\Delta t}\,\mathrm{skew}\left[\boldsymbol{H}_n^{-T}\boldsymbol{J}\right] + \hat{\boldsymbol{\Pi}}_{n+1}\right)M^T \tag{3.13}$$

and

$$B_n\left(2\,\mathrm{skew}\left[B_n^{-T}\right] - \hat{\pi}\right)B_n^T = M\left(\frac{4}{\Delta t}\,\mathrm{skew}\left[\mathbf{T}(\bar{\Theta})\mathbf{H}_n^{-T}\boldsymbol{J}\right] - \hat{\boldsymbol{\Pi}}_n\right)M^T. \tag{3.14}$$

Thus, since $\boldsymbol{H}_n$ is invertible for reasonable values of $\bar{\Theta}$, (3.12) is equivalent to the condition (3.5) and the proof is completed.

3.2. A New Exact Energy- and Momentum-Conserving and Symplectic Scheme

We now specialize the calculations of the preceding section to the one-parameter family of exact energy- and momentum-conserving algorithms identified in Result 4. We show below that the symplectic condition (3.5) yields

Result 5. *The energy-momentum preserving algorithm defined by (2.24) with* $\Theta = \kappa\left(|\bar{\Theta}|^2\right)\bar{\Theta}$ *defined by expression (2.28), that is,*

$$\hat{\Theta} := \Delta t\,\Omega_{n+(1/2)} = (\Delta t/2)\boldsymbol{J}^{-1}(\boldsymbol{\Pi}_n + \boldsymbol{\Pi}_{n+1}),$$

is symplectic if the function $\kappa\colon \mathbb{R} \to \mathbb{R}$ *satisfies the differential equation*

$$\frac{d\kappa}{dx} = \frac{\kappa^3}{4 - x\kappa^2}, \tag{3.15}$$

with explicit closed-form solution

$$\kappa(x) = \frac{2}{1 + \sqrt{1 - x}} = 1 + \tan^2\left(\frac{1}{2}\arcsin\sqrt{x}\right). \tag{3.16}$$

Observe that $\kappa(x)$ *is real valued only if* $0 \le x \le 1$. *This condition places the mild restriction* $|\bar{\Theta}| \le 1$, *that is,* $|\Delta t| \le 1/|\Omega_{n+(1/2)}|$, *on the admissible time steps.*

Comparing the general algorithm (3.3) with expressions (2.24) and (2.28), we see that the proof of the preceding result reduces to checking the symplectic condition (3.5) for the specific choice

$$\mathbf{T}(\Theta) = \mathrm{cay}[\Theta] \quad \text{with} \quad \Theta = \kappa\left(|\bar{\Theta}|^2\right)\bar{\Theta}. \tag{3.17}$$

Since the algorithm (2.24) is equivalent to the scheme (2.17) with $\alpha = \frac{1}{2}$, the right-hand side of the symplectic condition

$$\Pi_n - \Pi_{n+1} = \Theta \times \Pi_{n+(1/2)} = \frac{\kappa}{\Delta t}\bar{\Theta} \times J\bar{\Theta}. \tag{3.18}$$

Thus, it only remains to compute the left-hand side of (3.5) The linearized operator $\boldsymbol{H}_n$ associated with the transformation $\mathbf{T}$ is computed from (3.17) using the chain rule as

$$\boldsymbol{H}(\bar{\Theta})\delta\bar{\Theta} = \boldsymbol{H}_{\mathrm{cay}}(\Theta)\left(\kappa\delta\bar{\Theta} + 2\kappa'(\bar{\Theta}\cdot\delta\bar{\Theta})\bar{\Theta}\right) = \boldsymbol{H}_{\mathrm{cay}}(\Theta)\mathbb{P}(\bar{\Theta})\delta\bar{\Theta}, \tag{3.19}$$

where $\mathbb{P}(\bar{\Theta})$ is a scaled projection operator and $\boldsymbol{H}_{\mathrm{cay}}$ is the linearization of the Cayley transform, given by

$$\mathbb{P}(\bar{\Theta}) := \kappa\mathbf{1} + 2\kappa'\bar{\Theta}\otimes\bar{\Theta} \quad \text{and} \quad \boldsymbol{H}_{\mathrm{cay}}(\Theta)^{-T} = \mathbf{1} - \tfrac{1}{2}\bar{\Theta} + \tfrac{1}{4}\Theta\otimes\Theta. \tag{3.20}$$

Using the Sherman–Morrison formula, $\mathbb{P}(\bar{\Theta})$ can be explicitly inverted:

$$\mathbb{P}(\bar{\Theta})^{-1} = \frac{1}{\kappa}\left(\mathbf{1} + \frac{2\kappa'}{\kappa + 2|\bar{\Theta}|^2\kappa'}\bar{\Theta}\otimes\bar{\Theta}\right) = \frac{1}{\kappa}\left(\mathbf{1} + \frac{2\kappa'}{\kappa^3 + 2\kappa^2|\bar{\Theta}|^2\kappa'}\Theta\otimes\Theta\right). \tag{3.21}$$

As a result, the matrix $\boldsymbol{H}(\bar{\Theta})^{-T}$ appearing in the symplectic condition (3.5) satisfies

$$\boldsymbol{H}(\bar{\Theta})^{-T} = \boldsymbol{H}_{\mathrm{cay}}(\Theta)^{-T}\mathbb{P}(\bar{\Theta})^{-T} = \frac{1}{\kappa}\left(\mathbf{1} - \frac{1}{2}\bar{\Theta} + \mu\Theta\otimes\Theta\right), \tag{3.22}$$

where

$$\mu := \frac{1}{4}\left(1 - \frac{2\kappa'\left(4 + \kappa^2|\bar{\Theta}|^2\right)}{\kappa^3 + 2\kappa^2|\bar{\Theta}|^2\kappa'}\right). \tag{3.23}$$

Now a direct computation using the identity $\widehat{\Theta}^2 = \Theta \otimes \Theta - |\Theta|^2 \mathbf{1}$ yields

$$(\mathbf{1} + \mathbf{T}(\bar{\Theta}))\boldsymbol{H}(\bar{\Theta})^{-T} = 2\left(\mathbf{1} + \frac{1}{1 + |\Theta|^2/4}\left(\tfrac{1}{2}\hat{\bar{\Theta}} + \tfrac{1}{4}\hat{\Theta}^2\right)\right)\boldsymbol{H}(\bar{\Theta})^{-T}$$
$$= \frac{2}{\kappa}(\mathbf{1} + \mu\Theta \otimes \Theta). \tag{3.24}$$

Therefore, the left-hand-side of the symplectic condition (3.5) reduces to

$$\operatorname{skew}\left[(\mathbf{1} + \mathbf{T}(\Theta))\boldsymbol{H}(\Theta)^{-T}\boldsymbol{J}\right] = \frac{2\mu}{\kappa}\operatorname{skew}[\Theta \otimes \boldsymbol{J}\Theta] = \mu\kappa\boldsymbol{J}\Theta \times \Theta. \tag{3.25}$$

Comparing (3.25) with (3.18) we conclude that the symplectic condition (3.5) holds provided that $\mu = -\frac{1}{4}$, which yields the differential equation (3.15) and completes the proof.

3.3. Error Estimates

Having found an algorithm which exactly preserves the symplectic two-form, we now attempt to provide a measure of the extent to which the other algorithms considered *fail* to preserve it. The general formula for the Poisson error is derived in Section 5.3; we simply apply the formula to the algorithms (3.3).

The algorithmic approximation of the symplectic form at the nth time step is given by

$$\bar{\omega}_{n+1} := L_n^T \bar{\omega}_n L_n, \quad \text{where } \bar{\omega}_0 := \omega(\Lambda_0, \pi_0) \tag{3.26}$$

and L_n denotes the linearized equations at the nth step. The approximate symplectic form satisfies

$$\bar{\omega}_n = \frac{1}{1 - \pi \cdot \sigma_n}\begin{pmatrix} \hat{\pi} & \mathbf{1} - \sigma_n \otimes \pi \\ \pi \otimes \sigma_n - \mathbf{1} & \hat{\sigma}_n \end{pmatrix}, \quad \text{with inverse } \bar{\omega}_n^{-1} = \begin{pmatrix} \hat{\sigma}_n & -\mathbf{1} \\ \mathbf{1} & \hat{\pi} \end{pmatrix}, \tag{3.27}$$

for $\sigma_n \in \mathbb{R}^3$ defined inductively by $\sigma_0 := \mathbf{0}$ and

$$\sigma_{n+1} = \sigma_n + \frac{4}{\det N_n} N_n \operatorname{rot}[(\mathbf{1} + \hat{\pi}\hat{\sigma}_n)(N_n - \hat{\pi})], \tag{3.28}$$

where the map rot: $L(3) \to \mathbb{R}^3$ satisfies $\widehat{\operatorname{rot}[M]} = \frac{1}{2}(M - M^T)$ for any $M \in L(3)$ and the matrix N_n is given by

$$N_n := \Lambda_{n+1}\left(\frac{2}{\Delta t}\boldsymbol{H}(\bar{\Theta})^{-1}\boldsymbol{J} + \hat{\Pi}_{n+1}\right)\left(\mathbf{1} + \tfrac{1}{2}\hat{\Theta}\right)\Lambda_{n+1}^T. \tag{3.29}$$

We will monitor the numerical growth of the symplectic error for the following three algorithms involving scaled Cayley transformations:

1. *Cayley transform*: $\kappa(\bar{\Theta}) \equiv 1$.
2. *Exponential map*: $\kappa(\bar{\Theta}) = \tan\left(\frac{1}{2}|\bar{\Theta}|\right) \Big/ \left(\frac{1}{2}|\bar{\Theta}|\right)$.
3. *Symplectic algorithm*: $\kappa(\bar{\Theta}) = \frac{2}{1 + \sqrt{1 - |\theta|^2}}$.

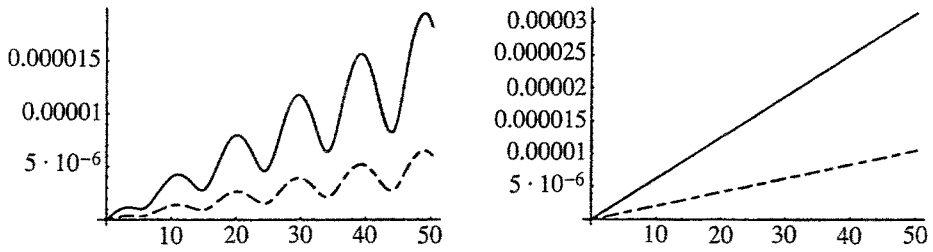

Fig. 1. Poisson errors for the Cayley transform (—) and exponential map (– –).

The plots given below were generated using the *Mathematica* code listed in Appendix A. We do not report results on the time histories of momentum and energy since they are conserved by design in the three algorithms. The results below demonstrate the exact symplectic character of the proposed algorithm and the superior performance of the exponential map (dashed line) in comparison to the Cayley transform (solid line).

All of the integrations shown in Figs. 1 and 2 were computed for a total of fifty units of time, with initial angular velocity (0.2, 0, 1). Both plots shown in Fig. 1 were computed using a time-step of 0.05. The plot on the left was computed using an asymmetric reference inertia tensor diag[1, 2, 3]; the one on the right used a symmetric inertia tensor diag[1, 1, 2]. The solid line traces the magnitude of the Poisson error for the Cayley transform; the dashed line traces the magnitude of the error for the exponential map. Figure 2 shows the maximum norm of the Poisson error and the maximum variation in the total energy for the simulations discussed above and for simulations using the same initial conditions, but a time-step of 0.005. The notation A indicates the simulations using the asymmetric reference inertia tensor diag[1, 2, 3], while S denotes the symmetric inertia tensor diag[1, 1, 2].

Poisson error				
	$\Delta t = .05$		$\Delta t = .005$	
Run	A	S	A	S
Symplectic	$1.9\ 10^{-14}$	$3.4\ 10^{-14}$	$2.5\ 10^{-14}$	$4.4\ 10^{-14}$
Exponential	$6.4\ 10^{-4}$	$1.0\ 10^{-3}$	$6.5\ 10^{-6}$	$1.0\ 10^{-5}$
Cayley	$1.9\ 10^{-3}$	$3.1\ 10^{-3}$	$1.9\ 10^{-5}$	$3.1\ 10^{-5}$
Energy change				
	$\Delta t = .05$		$\Delta t = .005$	
Run	A	S	A	S
Symplectic	$8.2\ 10^{-15}$	$9.7\ 10^{-15}$	$1.1\ 10^{-13}$	$2.0\ 10^{-13}$
Exponential	$2.7\ 10^{-15}$	$5.8\ 10^{-15}$	$2.3\ 10^{-14}$	$1.1\ 10^{-13}$
Cayley	$1.3\ 10^{-15}$	$1.4\ 10^{-14}$	$1.8\ 10^{-14}$	$5.8\ 10^{-14}$

Fig. 2. Maximum Poisson errors and energy changes.

All runs were computed using the default *Mathematica* precision of sixteen digits and accuracy goal of six digits on an SGI Indigo. It should be noted that the Poisson error for the symplectic scaling and the errors in the energy for all of the scalings are well within the range of round-off error. (The fact that the errors actually increase slightly when the time-step is decreased, resulting in an increase in the total number of steps taken over the total time interval, indicates that they are due to accumulated round-off error.)

4. Dynamics on the Rotation Group with Nonzero Potential

We shall now extend several of the results of the previous section to a large class of Hamiltonian systems with configuration manifold $SO(3)$. It does not, however, appear to be generally possible to conserve momentum, energy, and the symplectic form simultaneously using the class of general mid-point algorithms analogous to those developed in Section 2; for such algorithms, preservation of the symplectic form leads to conservation of kinetic energy, which is inconsistent with conservation of the total energy for systems possessing nonconstant potential energy. We consider Hamiltonian systems on $T^*SO(3)$ with a nontrivial potential which is invariant under spatial (right) rotations about an axis γ. The heavy top may be kept in mind as a prototype of such systems. We write the S^1 invariant potential in the form $V(\Lambda) = \widetilde{V}(\Lambda^T\gamma)$, where $\widetilde{V}: \mathbb{R}^3 \to \mathbb{R}$. Thus the first variation satisfies

$$DV(\Lambda)\cdot(\widehat{\delta\theta}\Lambda) = D\widetilde{V}(\Lambda^T\gamma)\cdot(\widehat{\delta\theta}\Lambda)^T\gamma = (\Lambda D\widetilde{V}(\Lambda^T\gamma))\cdot(\gamma\times\delta\theta). \tag{4.1}$$

Thus, we see that $DV(\Lambda) = -\gamma\times\mathbf{e}(\Lambda)$ for some function $\mathbf{e}: SO(3)\to\mathbb{R}^3$. The Hamiltonian equations associated to such a potential are

$$\left.\begin{aligned}\dot{\Lambda} &= \Omega\\ \dot{\pi} &= \gamma\times\mathbf{e}(\Lambda)\end{aligned}\right\}. \tag{4.2}$$

4.1. Conservation of Energy and Momentum

The unreduced Euler equations are a special case of (4.2) for which $\mathbf{e}(\Lambda)$ is equal to zero. We can generalize the algorithms (3.3) to include the case of nonzero $\mathbf{e}$. We carry out step one and two of the general program described in Section 2 by selecting the family of algorithms

$$\left.\begin{aligned}\Lambda_{n+1} &= \Lambda_n T_n\\ \pi_{n+1} &= \pi_n + \Delta t\gamma\times\mathbf{e}_n\end{aligned}\right\}, \tag{4.3}$$

for some $T_n\in SO(3)$ and $\mathbf{e}_n\in\mathbb{R}^3$.

The appropriate interpretation of conservation of momentum for the general system (4.2) is not the same as that for the Euler equations. In the presence of a nontrivial potential the spatial momentum typically varies in time; however, (4.2_2) implies that the component of the momentum parallel to the axis of symmetry γ is constant in

time. This is consistent with Noether's theorem, since the Hamiltonian $H(\Pi, \Lambda) = \frac{1}{2}|\Pi|^2_{\mathcal{G}^*} + V(\Lambda)$ is invariant only under spatial rotations about γ. The form of (4.3_2) guarantees that

Result 6. *The algorithms (4.3) conserve angular momentum about the axis γ for any choice of T_n and $\mathbf{e}_n$.*

We now turn to the conservation of energy, restricting our attention to algorithms of the form (4.3) for which

$$\left.\begin{aligned} T_n &= \mathbf{T}(\Theta) := \operatorname{cay}[\kappa(\Theta)\Theta] \\ \mathbf{e}_n &= \mathbf{e}(\Lambda_n, \Theta) \\ \Theta &:= \Delta t \Omega_{n+(1/2)} = \tfrac{\Delta t}{2} J^{-1}(\Pi_n + \Pi_{n+1}) \end{aligned}\right\} \tag{4.4}$$

for some functions $\kappa: \mathbb{R}^3 \to \mathbb{R}$ and $\mathbf{e} : SO(3) \times \mathbb{R}^3 \to \mathbb{R}^3$. The choice of algorithms (4.4) may not be essential for conservation of energy, but we believe that it is a very natural one. The use of the scaled Cayley transforms is suggested by the results of Section 2. Our choice of Θ is motivated both by the traditional success of the midpoint rule and by results given in Section 5 that suggest that the specification of energy-conserving algorithms is greatly simplified if $\mathbf{T}(\Theta)\Omega_{n+(1/2)} = \Omega_{n+(1/2)}$, which for the scaled Cayley transforms is equivalent to the condition that Θ is parallel to $\Omega_{n+(1/2)}$. If the rotation matrix $\mathbf{T}(\Theta)$ is viewed as an algorithmic approximation to rotation through $\Delta t \Omega_{n+(1/2)}$, then the condition $\mathbf{T}(\Theta)\Omega_{n+(1/2)} = \Omega_{n+(1/2)}$ has the simple physical interpretation of specifying that the algorithm must respect the axis, if not the magnitude, of the rotation.

Result 7. *The algorithms specified by (4.3) and (4.4) conserve energy if*

$$\kappa(\Theta)\gamma \cdot \Lambda_n \Theta \times \mathbf{e}(\Lambda_n, \Theta) = V(\Lambda_{n+1}) - V(\Lambda_n). \tag{4.5}$$

For the heavy top, with $V(\Lambda) = \gamma \cdot \Lambda E$ for some fixed vector $E \in \mathbb{R}^3$, energy is conserved if

$$\mathbf{e}(\Lambda_n, \Theta) = \tfrac{1}{2}\Lambda_n(\mathbf{1} + \mathbf{T}(\Theta))E = \tfrac{1}{2}(\Lambda_n + \Lambda_{n+1})E \tag{4.6}$$

for any choice of the scaling function $\kappa(\Theta)$; in particular, those considered in the preceding section.

Equation (2.26) suggests that we express the difference $\Pi_{n+1} - \Pi_n$, and thus the change in kinetic energy, in terms of Λ_n and Θ. The algorithm (4.3) implies that

$$\Pi_n = \mathbf{T}(\Theta)^T \Pi_{n+1} - \Delta t \Lambda_n^T(\gamma \times \mathbf{e}). \tag{4.7}$$

Substituting (4.7) into (4.4_3) and solving for Π_{n+1}, we obtain

$$\begin{aligned} \Pi_{n+1} - \Pi_n &= (\mathbf{1} - \mathbf{T}(\Theta))^T(\mathbf{1} + \mathbf{T}(\Theta))^{-T}\left(\tfrac{2}{\Delta t} J\Theta + \Delta t \Lambda_n^T(\gamma \times \mathbf{e})\right) + \Delta t \Lambda_n^T(\gamma \times \mathbf{e}) \\ &= \Delta t \kappa(\Theta)\left(\tfrac{1}{\Delta t^2}\Theta \times J\Theta + \left(\mathbf{1} + \tfrac{1}{2}\hat{\Theta}\right)\Lambda_n^T(\gamma \times \mathbf{e})\right) \end{aligned} \tag{4.8}$$

by means of the identity

$$(\mathbf{1} + \mathbf{T}(\Theta))^{-1}(\mathbf{T}(\Theta) - \mathbf{1}) = \tfrac{1}{2}\kappa(\Theta)\hat{\Theta}. \tag{4.9}$$

Equations (4.4$_3$) and (4.8) imply that

$$\begin{aligned} H_{n+1} - H_n &= \tfrac{1}{\Delta t}(\Pi_{n+1} - \Pi_n) \cdot \Theta + V(\Lambda_{n+1}) - V(\Lambda_n) \\ &= \kappa(\Theta)\gamma \times \mathbf{e} \cdot \Lambda_n \Theta + V(\Lambda_{n+1}) - V(\Lambda_n). \end{aligned} \tag{4.10}$$

Thus the total energy is conserved if and only if (4.5) holds.

We now turn to the example of a heavy top and use equation (4.5) to identify a family of energy conserving algorithms. The change in potential energy for the heavy top is

$$V(\Lambda_{n+1}) - V(\Lambda_n) = \gamma \cdot (\Lambda_{n+1} - \Lambda_n)E = \gamma \cdot \Lambda_n(\mathbf{T}(\Theta) - \mathbf{1})E. \tag{4.11}$$

Thus (4.5) implies that conservation of energy holds if

$$\kappa(\Theta)\gamma \cdot \Lambda_n \Theta \times \mathbf{e} = \gamma \cdot \Lambda_n(\mathbf{T}(\Theta) - \mathbf{1})E. \tag{4.12}$$

Using the identity $(\mathbf{T}(\Theta) - \mathbf{1}) = \frac{1}{2}\kappa(\Theta)\hat{\Theta}(\mathbf{1} + \mathbf{T}(\Theta))$, we see that $\mathbf{e}$ given by (4.6) satisfies (4.12).

4.2. Symplectic Conditions

Result 8. *The algorithms determined by (4.3) and (4.4) are symplectic if and only if condition (3.5) holds,*

$$\gamma \times \mathbf{e}(\Lambda_n, \Theta) = 0, \quad \textit{equivalently,} \quad \Pi_{n+1} - \Pi_n = \frac{1}{\Delta t}\Theta \times J\Theta, \tag{4.13}$$

and

$$\hat{\gamma} D\mathbf{e}(\Lambda_n, \Theta) \cdot (\widehat{\delta\theta}\Lambda_n, \delta\Theta) = \left(\frac{1}{2}\widehat{\mathbf{e}(\Lambda_n, \Theta)}\hat{\gamma} + S(\Lambda_n, \Theta)\right)\left(\delta\theta + \tfrac{1}{2}\Lambda_n\left(\mathbf{1} + \tfrac{1}{2}\hat{\Theta}\right)\boldsymbol{H}(\Theta)\delta\Theta\right) \tag{4.14}$$

for some symmetric matrix $S(\Lambda_n, \Theta)$. The condition (4.13) implies conservation of kinetic energy and the spatial momenta; it holds only if the algorithmic "force" equals zero.

We do not derive the symplectic conditions in detail here; rather, we sketch the principal steps here and refer to Section 5.2 for the detailed derivation of these conditions for a general Lie group. The derivation for the rotation group has many features in common with that given in Section 2 for the unreduced Euler equations.

The linearization of (4.3) is

$$(\delta\theta_{n+1}, \delta\pi_{n+1}) = \tilde{L}_{n+1}^{-1}\tilde{L}_n(\delta\theta_n, \delta\pi_n), \tag{4.15}$$

where

$$\tilde{L}_n := \begin{pmatrix} \mathbf{1} + B_n\hat{\pi}_n & B_n \\ A_n\hat{\pi}_n + \Delta t\, F_n & \mathbf{1} + A_n \end{pmatrix} \tag{4.16}$$

and

$$\tilde{L}_{n+1} := \begin{pmatrix} \mathbf{1} + B_{n+1}\hat{\pi}_{n+1} & B_{n+1} \\ A_{n+1}\hat{\pi}_{n+1} & \mathbf{1} + A_{n+1} \end{pmatrix}. \tag{4.17}$$

Here

$$\left.\begin{aligned} A_n &:= \tfrac{\Delta t^2}{2} G_n J^{-1} \Lambda_n^T, & A_{n+1} &:= -\tfrac{\Delta t^2}{2} G_n J^{-1} \Lambda_{n+1}^T \\ B_n &:= \tfrac{\Delta t}{2} \Lambda_{n+1} H(\Theta) J^{-1} \Lambda_n^T, & B_{n+1} &:= -\tfrac{\Delta t}{2} \Lambda_{n+1} H(\Theta) J^{-1} \Lambda_{n+1}^T \end{aligned}\right\}, \tag{4.18}$$

and F_n and $G_n \in L(3)$ are determined by the relationship

$$F_n \delta\theta + G_n \delta\Theta = \hat{\gamma} D\mathbf{e}(\Lambda_n, \Theta) \cdot (\widehat{\delta\theta} \Lambda_n, \delta\Theta) \tag{4.19}$$

for all $\delta\theta$, $\delta\Theta \in \mathbb{R}^3$.

As in the case of the free rigid body considered in Section 3.1, we express the test for symplecticity in the form

$$\tilde{L}_n \begin{pmatrix} \mathbf{0} & -\mathbf{1} \\ \mathbf{1} & \hat{\pi}_n \end{pmatrix} \tilde{L}_n^T = \tilde{L}_{n+1} \begin{pmatrix} \mathbf{0} & -\mathbf{1} \\ \mathbf{1} & \hat{\pi}_{n+1} \end{pmatrix} \tilde{L}_{n+1}^T. \tag{4.20}$$

Equation (4.20) is equivalent to the conditions

1. $B_{n+1}\hat{\pi}_{n+1}B_{n+1}^T - B_n\hat{\pi}_n B_n^T = 2\,\mathrm{skew}[B_{n+1} - B_n]$
2. $A_{n+1}\left(\hat{\pi}_{n+1}B_{n+1}^T - \mathbf{1}\right) - A_n\left(\hat{\pi}_n B_n^T - \mathbf{1}\right) = \Delta t\, F_n B_n^T$
3. $A_{n+1}\hat{\pi}_{n+1}A_{n+1}^T - A_n\hat{\pi}_n A_n^T = \Delta t\, \left(\widehat{\gamma \times \mathbf{e}} + 2\,\mathrm{skew}\left[F_n(\mathbf{1} + A_n)^T\right]\right)$.

These conditions can be sequentially simplified to obtain the conditions given in Result 8. The first condition is identical to that appearing in the free rigid body case. The second symplectic condition can be written as

$$G_n H(\Theta)^{-1}(\mathbf{T}(\Theta) + \mathbf{1})^T = F_n \Lambda_n; \tag{4.21}$$

the third condition simplifies to

$$\gamma \times \mathbf{e} + 2\,\mathrm{rot}[F_n] = 0. \tag{4.22}$$

Combining these conditions yields (4.14) It is a direct consequence of (4.10) that conservation of kinetic energy is implied by (4.8).

5. Algorithms on General Lie Groups

We now consider algorithms on general Lie groups. We shall initially restrict our attention to the Euler equations, for which the Hamiltonian is equal to the kinetic energy determined by a metric on the Lie algebra. We shall follow a slightly different

program than that used in the derivation of the algorithms for the rotation group. Guided by our results for that particular case, we shall combine the first two steps, assuming the existence of a map which allows us to carry out Step 2. We emphasize that the explicit identification of such a map for an arbitrary Lie group appears to be a nontrivial task. We do not attempt to carry out that task here. Rather, we shall construct a family of energy- and momentum-conserving algorithms assuming the existence of an approximate exponential map. We derive an explicit formula for the *Poisson error*, which provides a measure of the extent to which an algorithm fails to be symplectic, for a large class of algorithms. This formula can be used to determine symplectic algorithms on general Lie groups. The derivation of these results is analogous to those given for the algorithms on $SO(3)$ discussed in Section 2 and Section 5, hence several of these derivations have been relegated to Appendix B.

5.1. The Dynamics on a General Lie Group

We now briefly discuss some of the fundamental constructs relevant to Hamiltonian dynamics on a Lie group. For detailed discussions of these and related constructions, see, for example, Abraham and Marsden [1978] or Arnold [1988]. Given a Lie group G, we denote the Lagrangian coordinates on the cotangent bundle T^*G by $z = (q, p)$.

5.1.1. The Lie Algebra and Its Dual. The tangent space to G at the identity, that is, the space of infinitesimal group elements, is denoted by $\mathcal{G}$; its dual is denoted by $\mathcal{G}^*$. The exponential map $\exp: \mathcal{G} \to G$ maps infinitesimal motions to full group motions. We emphasize that while the exponential map can be expressed as a formal power series for all groups, relatively few Lie groups possess an exponential map for which an explicit closed form expression is known. Some examples are the rotation groups $SO(2)$ and $SO(3)$, the special linear group $SL(2)$ on $\mathbb{R}^2$, and, of course, additive groups.

5.1.2. Pairings. The natural dual pairing between the Lie algebra $\mathcal{G}$ and its dual $\mathcal{G}^*$ is denoted by $\langle\ ,\ \rangle$, for example, $\langle \mu, \xi \rangle$ for $\xi \in \mathcal{G}$ and $\mu \in \mathcal{G}^*$. We assume the existence of a metric on $\mathcal{G}$, denoted by $\langle\langle\ ,\ \rangle\rangle_{\mathcal{G}}$. The metric induces a map $\mathbf{m}: \mathcal{G} \to \mathcal{G}^*$, defined by

$$\langle \mathbf{m}\,\xi, \eta \rangle = \langle\langle \xi, \eta \rangle\rangle_{\mathcal{G}} \tag{5.1}$$

for all $\xi, \eta \in \mathcal{G}$, and a metric $\langle\langle\ ,\ \rangle\rangle_{\mathcal{G}^*}$ on $\mathcal{G}^*$, defined by

$$\langle\langle \mu, \nu \rangle\rangle_{\mathcal{G}^*} := \left\langle\left\langle \mathbf{m}^{-1}\mu, \mathbf{m}^{-1}\nu \right\rangle\right\rangle_{\mathcal{G}} \tag{5.2}$$

for all $\mu, \nu \in \mathcal{G}^*$.

5.1.3. Group Actions and Tangent Maps. The group G acts on itself on both the left and the right by group multiplication. We let L_q denote left multiplication by q, that is, $L_q \tilde{q} = q\tilde{q}$. Similarly, right multiplication by q is denoted by $R_q \tilde{q} := \tilde{q}q$. The adjoint action of G on $\mathcal{G}$ is given by

$$\mathrm{Ad}_q \xi = \left.\frac{d}{d\epsilon}\right|_{\epsilon=0} \exp(\epsilon\xi) q^{-1}. \tag{5.3}$$

The coadjoint action of G on $\mathcal{G}^*$ maps the dual of the algebra into itself and is determined by the relationship $\langle \mathrm{Ad}_q^* \mu, \xi \rangle = \langle \mu, \mathrm{Ad}_q \xi \rangle$ for all $q \in G$, $\xi \in \mathcal{G}$, and $\mu \in \mathcal{G}^*$. The infinitesimal adjoint and coadjoint actions of $\mathcal{G}$ on $\mathcal{G}$ and $\mathcal{G}^*$ are determined by the relations

$$\mathrm{ad}_\nu \xi = \left.\frac{d}{d\varepsilon}\right|_{\varepsilon=0} \mathrm{Ad}_{\exp(\varepsilon\eta)} \xi \quad \text{and} \quad \langle \mathrm{ad}_\eta^* \mu, \xi \rangle = \langle \mu, \mathrm{ad}_\eta \xi \rangle \tag{5.4}$$

for all $\xi, \eta \in \mathcal{G}$ and $\mu \in \mathcal{G}^*$.

5.1.4. Trivializations. T^*G can be represented by either the right or left trivialization. The left trivialization $T^*G \approx G \times \mathcal{G}^*$ is given by

$$(q, p) \mapsto (q, \Pi), \quad \text{where } \Pi := T_q^* L_q p. \tag{5.5}$$

The right trivialization $T^*G \approx G \times \mathcal{G}^*$ is given by

$$(q, p) \mapsto (q, \pi), \quad \text{where } \pi := T_q^* R_q p. \tag{5.6}$$

For matrix groups left (right) translation is simply matrix multiplication on the left (right).

5.1.5. The Symplectic Form. The canonical symplectic two-form on the cotangent bundle T^*G is most conveniently expressed with respect to the left or right trivialized variables. The symplectic form ω_L on $G \times \mathcal{G}^* \approx T^*G$ with respect to the left trivialization is given by

$$\omega_L(q, \Pi) = \begin{pmatrix} A & \mathbf{1} \\ -\mathbf{1} & \mathbf{0} \end{pmatrix}, \quad \text{with inverse} \quad \omega_L(q, \Pi)^{-1} = \begin{pmatrix} \mathbf{0} & -\mathbf{1} \\ \mathbf{1} & A \end{pmatrix}, \tag{5.7}$$

where $A : \mathcal{G} \to \mathcal{G}^*$ is determined by the relationship

$$A\xi := -\mathrm{ad}_\xi^* \Pi. \tag{5.8}$$

The symplectic form ω_R with respect to the right trivialization is given by

$$\omega_R(q, \pi) = \begin{pmatrix} \alpha & \mathbf{1} \\ -\mathbf{1} & \mathbf{0} \end{pmatrix}, \quad \text{with inverse} \quad \omega_R(q, \pi)^{-1} = \begin{pmatrix} \mathbf{0} & -\mathbf{1} \\ \mathbf{1} & \alpha \end{pmatrix}, \tag{5.9}$$

where $\alpha : \mathcal{G} \to \mathcal{G}^*$ is determined by the relationship

$$\alpha\xi := \mathrm{ad}_\xi^* \pi. \tag{5.10}$$

The right trivialized representation of the symplectic form is derived by taking the variation of the equation $\pi = T^* R_q p$, yielding

$$\delta\pi = T_q^* R_q \delta p + (T_q(T_q^* R_q)\delta q) p, \tag{5.11}$$

where $T_q(T_q^*R_q) : T_qG \to L(T_q^*G, \mathfrak{g}^*)$. Solving (5.11) for δp and substituting the result into the canonical symplectic two-form on T^*G, we obtain

$$\begin{aligned}
&\omega(q,p)((T_qR_q\delta q, \delta p), (T_qR_q\Delta q, \Delta p)) \\
&\quad = \langle T_e^*R_{q^{-1}}(\Delta\pi - (T_q(T_q^*R_q)\Delta q)p), T_qR_q\delta q\rangle \\
&\qquad - \langle T_e^*R_{q^{-1}}(\delta\pi - (T_q(T_q^*R_q)\delta q)p), T_qR_q\Delta q\rangle \\
&\quad = \langle \Delta\pi, \delta q\rangle - \langle \delta p, \Delta q\rangle \\
&\qquad + \langle \pi, (T_q(T_qR_q)\delta q)\Delta q - (T_q(T_qR_q)\Delta q)\delta q\rangle \\
&\quad = \langle \Delta\pi, \delta q\rangle - \langle \delta p, \Delta q\rangle + \langle \pi, \mathrm{ad}_{\Delta q}\delta q\rangle. \qquad (5.12)
\end{aligned}$$

The derivation of the left-trivialized symplectic form is analogous.

5.1.6. The Unreduced Euler Equations. The Euler equations and unreduced Euler equations for a free rigid body are given by (2.12$_2$) and (2.12), respectively. As pointed out in Arnold [1988], essentially identical equations govern the dynamics on any Lie group whose Lie algebra is endowed with a metric. (The generalized Euler equations are often referred to as the Lie–Poisson equations.) The generalized unreduced Euler equations in 'body', i.e. left-trivialized coordinates, are

$$\left.\begin{aligned}
\dot{q} &= T_eL_q\Omega \\
\dot{\Pi} &= \mathrm{ad}^*_\Omega\Pi \\
\Omega &= \mathbf{m}^{-1}\Pi
\end{aligned}\right\}. \qquad (5.13)$$

Equations (5.13) can also be written in terms of the right-trivialized variables, yielding

$$\left.\begin{aligned}
\dot{q} &= T_eL_q\Omega \\
\dot{\pi} &= 0 \\
\Omega &= \mathbf{m}^{-1}\mathrm{Ad}^*_q\pi
\end{aligned}\right\}. \qquad (5.14)$$

5.1.7. The Hamiltonian. The flow determined by the generalized Euler equations conserves the energy

$$H(q,p) := \tfrac{1}{2}\|p\|^2_{T^*G}, \qquad (5.15)$$

where the inner product $\langle\langle\ ,\ \rangle\rangle_{T^*G}$ is determined by

$$\langle\langle p_1, p_2\rangle\rangle_{T^*G} = \langle\langle T_q^*L_qp_1, T_q^*L_qp_2\rangle\rangle_{\mathfrak{g}^*} \qquad (5.16)$$

for all $q \in G$ and all $p_1, p_2 \in T_q^*G$. The Hamiltonian (5.15) can also be written in terms of the left and right trivializations, namely

$$H(q,p) = H_L(q,\Pi) = H_R(q,\pi), \qquad (5.17)$$

where

$$H_L(q, \Pi) := \tfrac{1}{2}\|\Pi\|^2_{\mathcal{G}^*} \quad \text{and} \quad H_R(q, \pi) := \tfrac{1}{2}\|\mathrm{Ad}^*_q \pi\|^2_{\mathcal{G}^*}. \tag{5.18}$$

In fact, equations (5.13) are Hamiltonian; they can be written in the form

$$(\dot{q}, \dot{\Pi}) = \omega_L(q, \Pi)^{-1} DH_L(q, \Pi). \tag{5.19}$$

Similarly, (5.14) can be written as

$$(\dot{q}, \dot{\pi}) = \omega_R(q, \pi)^{-1} DH_R(q, \pi). \tag{5.20}$$

We note that the right-invariant Hamiltonian $\frac{1}{2}\|\pi\|^2_{\mathcal{G}^*}$ generates the "spatial" form of the unreduced Euler equations. The spatial form of the Euler equations is associated with systems such as the Euler equations for an incompressible fixed boundary perfect fluid, which have a right (body) symmetry.

5.1.8. Momentum Maps. The Hamiltonian (5.15) is invariant under the left action of G on itself; hence Noether's theorem states that the left momentum map should be conserved by the Hamiltonian flow. This can be seen directly from (5.21) and (5.14_2).

The momentum maps associated to the left and right actions of G on itself are

$$\Phi_L(q, p) = T^*_q R_q p = \pi \quad \text{and} \quad \Phi_R(q, p) = T^*_q L_q p = \Pi. \tag{5.21}$$

As an example, we shall identify some of the constructions defined above for the rotation group. The rotation group $SO(3)$ has Lie algebra $so(3) \approx \mathbb{R}^3$, with dual $so(0)^* \approx \mathbb{R}^3$. This is seen by varying the equation $\Lambda^T\Lambda = \mathbf{1}$ with respect to Λ, yielding $\mathrm{skew}[\Lambda^T\delta\Lambda] = \mathbf{0}$, that is, $\delta\Lambda = \widehat{\delta\Theta}\Lambda$ for some $\delta\Theta \in \mathbb{R}^3$. The natural pairing between the algebra and its dual is simply the Euclidean inner product. $SO(3)$ acts on itself by matrix multiplication on the right and left; straightforward calculations show that

$$\mathrm{Ad}_\Lambda \xi = \Lambda\xi, \quad \mathrm{Ad}^*_\Lambda \mu = \Lambda^T\mu, \quad \mathrm{ad}_\eta \xi = \eta \times \xi, \quad \text{and} \quad \mathrm{ad}^*_\eta \mu = \mu \times \eta. \tag{5.22}$$

Using these expressions, the remaining constructions discussed in Section 2 can readily be obtained from the general formulas given above.

5.2. Conserving Algorithms for the Unreduced Euler Equations

We shall construct algorithms for Hamiltonian systems on general Lie groups which capture as many as possible of the properties of the algorithms developed for the rotation group. To do so, we shall make use of the geometric constructions mentioned in the previous section which generalize the familiar constructs, such as rotations and cross products, associated with $SO(3)$. In addition, we must identify appropriate generalizations of the *algorithmic* constructions used in Sections 2 through 4. The existence of maps $\mathbf{T} : \mathbb{R}^3 \to SO(3)$ such as the scaled Cayley transforms was crucial for the construction of the algorithms (3.3) for the rotation group. In constructing algorithms on general Lie groups, we shall assume that an explicit map $\tau : \mathcal{G} \to G$

from the Lie algebra to the group is known. The map τ will play the role taken by the map $\mathbf{T}$ for the rotation group—it is an algorithmic approximation of the exponential map. Consistency requires that $\tau(\mathbf{0}) = \mathbf{1}$.

We consider algorithms of the form

$$\left.\begin{aligned} q_{n+1} &= L_{q_n}\tau(\Theta) \\ \pi_{n+1} &= \pi_n \\ \Theta &:= \Theta(\Delta t, \Omega_{n+1}, \Omega_n) \end{aligned}\right\}. \tag{5.23}$$

where

$$\Omega_n = \mathbf{m}^{-1}\Pi_n = \mathbf{m}^{-1}\mathrm{Ad}^*_{q_n}\pi_n \quad \text{and} \quad \Omega_{n+1} = \mathbf{m}^{-1}\Pi_{n+1} = \mathbf{m}^{-1}\mathrm{Ad}^*_{q_{n+1}}\pi_{n+1}. \tag{5.24}$$

Conservation of the right-trivialized momentum π is explicitly incorporated in the algorithms (5.23). The map $(q, p) \mapsto \pi$ is the momentum map associated to the left action of G on itself; hence

Result 9. *The algorithms (5.23) conserve the left (spatial) momentum map for any choice of* Θ *and* τ.

A straightforward calculation, given in Appendix B, shows that the algorithms (5.23) conserve energy if and only if

$$\left\langle \mathbf{m}\Omega_{n+(1/2)}, \left(2\left(\mathbf{1} + \mathrm{Ad}_{\tau(\Theta)}\right)^{-1} - \mathbf{1}\right)\Omega_{n+(1/2)} \right\rangle = 0. \tag{5.25}$$

A convenient and geometrically motivated condition which implies (5.25) relates the map τ, the vector Θ, and the average velocity $\Omega_{n+(1/2)}$:

Result 10. *A sufficient condition for the conservation of energy is that*

$$\mathrm{Ad}_{\tau(\Theta)}\Omega_{n+(1/2)} = \Omega_{n+(1/2)}. \tag{5.26}$$

The exponential map $\exp : \mathcal{G} \to G$ satisfies $\mathrm{Ad}_{\exp(\Theta)}\Theta = \Theta$ for all $\Theta \in \mathcal{G}$. If this property is shared by the map τ, that is, if $\mathrm{Ad}_{\tau(\Theta)}\Theta = \Theta$ for all $\Theta \in \mathcal{G}$, then one family of algorithms satisfying (5.25) is the generalized midpoint rule, determined by the condition

$$\Theta := \Delta t\Omega_{n+(1/2)}. \tag{5.27}$$

The algorithm determined by (5.23) and (5.27) is the general Lie group expression for the algorithm (3.3) discussed in Section 2.

We now specify conditions which will ensure that the general momentum-preserving algorithm determined by (5.23) and (5.27) is symplectic. Define $\boldsymbol{H} : \mathcal{G} \to L(\mathcal{G}, \mathcal{G})$ by

$$\boldsymbol{H}(\Theta) := TL_{\tau(\Theta)^{-1}}D\tau(\Theta). \tag{5.28}$$

The algorithm (5.23) has linearization

$$\begin{pmatrix} \delta q_{n+1} \\ \delta \pi_{n+1} \end{pmatrix} = \begin{pmatrix} \mathbf{1} + C_n \alpha & C_n \\ \mathbf{0} & \mathbf{1} \end{pmatrix} \begin{pmatrix} \delta q_n \\ \delta \pi_n \end{pmatrix}, \tag{5.29}$$

where, for invertible $\boldsymbol{H}(\Theta)$, $C_n : \mathcal{G}^* \to \mathcal{G}$ satisfies

$$C_n = \mathrm{Ad}_{q_{n+1}} \left(\frac{2}{\Delta t} \mathbf{m}\boldsymbol{H}(\Theta)^{-1} - \mathrm{ad}^* \Pi_{n+1} \right)^{-1} \left(\mathrm{Ad}^*_{q_n} + \mathrm{Ad}^*_{q_{n+1}} \right). \tag{5.30}$$

Result 11. *The algorithm (5.23), with Θ defined by (5.27), is symplectic if*

$$\frac{4}{\Delta t} \mathrm{skew}\left[\mathbf{m}\boldsymbol{H}(\Theta)^{-1} \left(\mathbf{1} + \mathrm{Ad}_{\tau(\Theta)} \right) \right] = \mathrm{ad}^* \left(\Pi_{n+1} - \Pi_n \right), \tag{5.31}$$

where for $M : \mathcal{G}^* \to \mathcal{G}$,

$$\langle \mu \ \mathrm{skew}[M] \nu \rangle := \tfrac{1}{2} \left(\langle \mu, M\nu \rangle - \langle \nu, M\mu \rangle \right) \tag{5.32}$$

for all $\mu, \nu \in \mathcal{G}^*$. The right-hand side of (5.31) can be expressed in terms of Θ using the relationship

$$\Pi_{n+1} - \Pi_n = \frac{4}{\Delta t} \left(\left(\mathbf{1} + \mathrm{Ad}^*_{\tau(\Theta)^{-1}} \right)^{-1} - \tfrac{1}{2} \mathbf{1} \right) \mathbf{m}\Theta_n. \tag{5.33}$$

Remark. If the group is abelian, then (5.31) simplifies to $\boldsymbol{H}(\Theta)^* \mathbf{m} = \mathbf{m}\boldsymbol{H}(\Theta)$.

5.3. Error Estimates

In theory, condition (5.31) can be used to determine symplectic algorithms. However, this condition may be difficult to explicitly implement. For some Lie groups, no explicit closed-form expression for a map $\tau : \mathcal{G} \to G$ is known; even in cases where such maps exist, they may fail to satisfy the symplectic condition. Thus, we may wish to use the preceding calculations to estimate the extent to which an algorithm for the unreduced Euler equations fails to be symplectic. It appears to be convenient to explicitly estimate the error in the Poisson matrix (i.e., the inverse of the symplectic matrix) and then relate the error in the Poisson matrix to the error in the symplectic form.

We define the approximate Poisson matrix $\mathcal{P}_{n+1}$ at the $(n+1)$th time-step by

$$\mathcal{P}_{n+1} := L_n \mathcal{P}_n L_n^*, \quad \text{where} \quad \mathcal{P}_0 := \omega(q_0, p_0)^{-1} = \begin{pmatrix} \mathbf{0} & -\mathbf{1} \\ \mathbf{1} & \alpha \end{pmatrix} \tag{5.34}$$

and the matrix L_n is given by (5.29).

Using the identity (3.10), we see that for the class of algorithms given in (5.23),

$$\mathcal{P}_n = \begin{pmatrix} \sigma_n & -\mathbf{1} \\ \mathbf{1} & \alpha \end{pmatrix}, \tag{5.35}$$

where $\sigma_0 := 0$ and $\sigma_n : \mathfrak{G}^* \to \mathfrak{G}$ is defined inductively by

$$\sigma_{n+1} := \sigma_n + \operatorname{skew}\Big[C_n(\mathbf{1} + \alpha\sigma_n)\big(2\mathbf{1} - \alpha C_n^*\big)\Big]. \tag{5.36}$$

Note that the error occurs only in the $\delta\pi$–$\delta\pi$ component of the approximate Poisson matrices $\mathcal{P}_n$. We shall refer to σ_n as the *Poisson error* at time-step n.

For the rotation group, if we identify the skew-symmetric map $\sigma_n : \mathbb{R}^3 \to \mathbb{R}^3$ with a three-vector, then the formula (5.36) for the Poisson error takes the form

$$\hat{\sigma}_{n+1} = \hat{\sigma}_n + C_n \operatorname{skew}\Big[(\mathbf{1} + \hat{\pi}\hat{\sigma}_n)\big(2C_n^{-T} - \hat{\pi}\big)\Big]C_n^T, \tag{5.37}$$

where the matrix C_n is given by

$$C_n = \Lambda_{n+1}\left(\frac{2}{\Delta t}\boldsymbol{J}\boldsymbol{H}(\Theta)^{-1} - \widehat{\Pi}_{n+1}\right)^{-1}(\mathbf{1} + \mathbf{T}(\Theta))\Lambda_{n+1}^T, \tag{5.38}$$

with inverse transpose

$$C_n^{-T} = \Lambda_{n+1}\left(\frac{1}{\Delta t}\boldsymbol{H}(\Theta)^{-T}\boldsymbol{J} + \tfrac{1}{2}\widehat{\Pi}_{n+1}\right)\left(\mathbf{1} + \frac{1}{2}\widehat{\Theta}\right)\Lambda_{n+1}^T. \tag{5.39}$$

Thus, using the identity

$$M\hat{\mathbf{x}}M^T = \det M\,\widehat{M^{-T}\mathbf{x}} \tag{5.40}$$

for $M \in GL(3)$ and $\mathbf{x} \in \mathbb{R}^3$, we obtain the formula (3.28) given in Section 3.3.

5.4. Algorithms for General Hamiltonians on Lie Groups

In Section 2 and Section 5.2, we considered only the unreduced Euler equations, for which the Hamiltonian is equal to the kinetic energy of the system. We now consider a system on T^*G with a nontrivial potential $V: G \to \mathbb{R}$. The canonical Hamiltonian equations associated with such a potential are

$$\left.\begin{aligned} \dot{q} &= \Omega \\ \dot{p} &= -DV(q) \end{aligned}\right\}. \tag{5.41}$$

We shall generalize the algorithms developed in Sections 2 and 5 so as to model equations (5.41) by incorporating an appropriate expression for the differential of the potential into the momentum update equation. A nontrivial potential breaks the symmetry of the system; we let $\widetilde{G}$ denote the (possibly trivial) symmetry group of the Hamiltonian

$$H(q,p) = \tfrac{1}{2}\|p\|^2_{T^*G} + V(q). \tag{5.42}$$

Invariance of the potential V under the action of $\widetilde{G}$ implies that $DV(q) \in (\tilde{\mathfrak{G}} \cdot q)^A$, the annihilator of the tangent to the group orbit.

We consider algorithms associated with (4.2) of the form

$$\left.\begin{aligned} q_{n+1} &= q_n\tau(\Theta) \\ \pi_{n+1} &= \pi_n + \Delta t\mathcal{F}(q_n, \Theta) \\ \Theta &= \Theta(\Delta t, \Pi_n, \Pi_{n+1}) \end{aligned}\right\}. \tag{5.43}$$

We do not give general conditions for conservation of momentum here, since such conditions depend strongly on the action of the symmetry group. However, we consider two special but common cases—first, the case in which the symmetry group $\tilde{G}$ is a subgroup of G, acting by left multiplication, and second, a particular case in which the configuration group G is additive and the symmetry group $\tilde{G}$ acts linearly on G. In the first case, the condition for conservation of momentum is simply that $\mathcal{F}(q_n, \Theta) \in \tilde{\mathcal{G}}^A \subset \mathcal{G}^*$; that is,

$$\langle \mathcal{F}(q_n, \Theta), \eta \rangle = 0 \qquad \text{for all } \eta \in \tilde{\mathcal{G}}, \tag{5.44}$$

where $\tilde{\mathcal{G}}$ denotes the Lie algebra of the subgroup $\tilde{G}$. We next consider the special class of algorithms on a linear group for which τ is the identity map and Θ is a convex combination of the body velocities; that is,

$$\Theta = \mathbf{m}^{-1}(\alpha p_{n+1} + (1 - \alpha)p_n) \tag{5.45}$$

for some $\alpha \in [0, 1]$. For $\xi \in \tilde{\mathcal{G}}$, we let $\hat{\xi} : G \approx \mathcal{G} \to \mathcal{G}$ denote the map determined by the infinitesimal group action. This notation is intended to be suggestive of the map from $\mathbb{R}^3$ to the space of three by three skew matrices associated with the action of $SO(3)$ on matrix groups, which is the motivation for our treatment of this special case.

Result 12. *The momentum for a linear Lie group is conserved if and only if* $\mathcal{F}(q_n, \Theta) \in (\tilde{\mathcal{G}} \cdot q_{n+(1-\alpha)})^A$*; that is,*

$$\langle \mathcal{F}(q_n, \Theta), \hat{\xi} q_{n+(1-\alpha)} \rangle = 0 \tag{5.46}$$

for all $\xi \in \tilde{\mathcal{G}}$.

The momentum map $\Phi : T^*G \to \tilde{\mathcal{G}}^*$ is determined by the relationship

$$\langle \Phi(q, p), \xi \rangle = \langle p, \hat{\xi} q \rangle \tag{5.47}$$

for all $(q, p) \in T^*G$ and $\xi \in \tilde{\mathcal{G}}$. The change in momentum satisfies

$$\begin{aligned} &\langle \Phi(q_{n+1}, p_{n+1}) - \Phi(q_n, p_n), \xi \rangle \\ &\quad = \langle p_{n+1} - p_n, \hat{\xi} q_{n+(1-\alpha)} \rangle + \langle p_{n+\alpha}, \hat{\xi}(q_{n+1} - q_n) \rangle \\ &\quad = \Delta t \langle \mathcal{F}(q_n, \Theta), \hat{\xi} q_{n+(1-\alpha)} \rangle + \langle p_{n+\alpha}, \hat{\xi} p_{n+\alpha} \rangle_{\mathcal{G}^*}. \end{aligned} \tag{5.48}$$

In the linear case $\tilde{G}$-invariance of H implies that $\tilde{G}$ is a subgroup of the group of isometries of $\langle\langle\ ,\ \rangle\rangle_{T^*G}$; hence $\langle\langle p_{n+\alpha}, \hat{\xi} p_{n+\alpha} \rangle\rangle_{\mathcal{G}^*} = 0$.

Result 13. *Conservation of energy holds if* $\mathrm{Ad}_{\tau(\Theta)}\Omega_{n+(1/2)} = \Omega_{n+(1/2)}$ *and*

$$\Delta t\langle \mathcal{F}(q_n, \Theta), \mathrm{Ad}_{q_n}\Omega_{n+(1/2)}\rangle = V(q_n) - V(q_{n+1}). \tag{5.49}$$

A more general, but substantially more complicated, energy conservation condition is given in Appendix B.

We shall now specify conditions under which the algorithm (5.43) for a Hamiltonian system with a nontrivial potential is symplectic. To simplify the necessary expressions, we introduce the following notation. Define F_n and $G_n \in L(\mathcal{G}, \mathcal{G}^*)$ by

$$F_n\delta q + G_n\delta\Theta = D\mathcal{F}(q_n, \Theta)\cdot(T_eR_{q_n}\delta q, \delta\Theta) \tag{5.50}$$

for all δq_n, $\delta\Theta \in \mathcal{G}$ and Ψ_n and $\Psi_{n+1} : \mathcal{G}^* \to \mathcal{G}$ by

$$D\Theta(\Delta t, \Omega_n, \Omega_{n+1})\cdot(0, \mathbf{m}^{-1}\delta\Pi_n, \mathbf{m}^{-1}\delta\Pi_{n+1}) = \Psi_n\delta\Pi_n + \Psi_{n+1}\delta\Pi_{n+1} \tag{5.51}$$

for all $\delta\Pi_n$ and $\delta\Pi_{n+1} \in \mathcal{G}^*$.

Result 14. *The algorithm (5.43) is symplectic if*

1. $\dfrac{2}{\Delta t}\,\mathrm{skew}\left[H(\Theta)^{-1}\left(\Psi_{n+1}^* + \mathrm{Ad}_{\tau(\Theta)^{-1}}\Psi_n^*\right)\right] = \Psi_{n+1}\mathrm{ad}^*\Pi_{n+1}\Psi_{n+1}^* - \Psi_n\mathrm{ad}^*\Pi_n\Psi_n^*$
2. $G_nH(\Theta)^{-1}\left(\Psi_{n+1}^* + \mathrm{Ad}_{\tau(\Theta)^{-1}}\Psi_n^*\right) = F_n\mathrm{Ad}_{q_n}\Psi_n^*$
3. $\mathrm{ad}^*\mathcal{F}(q_n, \Theta) = -2\,\mathrm{skew}[F_n]$.

Note that there are *three* sets of conditions to be satisfied, corresponding to three components of the Poisson matrix, in comparison to the single condition associated with the $\delta\pi$–$\delta\pi$ component of the Poisson matrix which arose in the case of the Euler equations.

In special cases, the conditions given in Result 14 can be further simplified: if Θ is given by (5.27), then the first two symplectic conditions take the form

1′. $\dfrac{4}{\Delta t}\,\mathrm{skew}\left[H(\Theta)^{-1}\left(\mathbf{1} + \mathrm{Ad}_{\tau(\Theta)^{-1}}\right)\right] = \mathrm{ad}^*(\Pi_{n+1} - \Pi_n)$

2′. $D\mathcal{F}(q_n, \Theta)\cdot(\delta q, \delta\Theta) = F_n\left(\delta q + \left(\mathbf{1} + \mathrm{Ad}_{\tau(\Theta)^{-1}}\right)^{-1}H(\Theta)\mathrm{Ad}_{q_n}\delta\Theta\right)$.

If the group is abelian, then the symplectic conditions simplify dramatically. If $\mathcal{F}(q_n, \Theta) = \check{\mathcal{F}}(q_n, q_{n+1})$ for some map $\check{\mathcal{F}} : G\times G \to \mathcal{G}$ with first variation satisfying

$$D\check{\mathcal{F}}(q_n, q_{n+1})\cdot(T_eL_{q_n}\delta q_n, T_eL_{q_{n+1}}\delta q_{n+1}) = \frac{\delta\check{\mathcal{F}}}{\delta q_n}\delta q_n + \frac{\delta\check{\mathcal{F}}}{\delta q_{n+1}}\delta q_{n+1} \tag{5.52}$$

for some $\frac{\delta\check{\mathcal{F}}}{\delta q_n}$, $\frac{\delta\check{\mathcal{F}}}{\delta q_{n+1}} \in L(\mathcal{G}, \mathcal{G}^*)$ and all δq_n, $\delta q_{n+1} \in \mathcal{G}$, then

$$F_n = \frac{\delta\check{\mathcal{F}}}{\delta q_n} + \frac{\delta\check{\mathcal{F}}}{\delta q_{n+1}} \quad \text{and} \quad G_n = \frac{\delta\check{\mathcal{F}}}{\delta q_{n+1}}H(\Theta). \tag{5.53}$$

Hence the symplectic conditions for an abelian group are equivalent to the conditions

$$1''.\ \text{skew}\,[\boldsymbol{H}(\Theta)\,(\Psi_{n+1}+\Psi_n)] = 0$$

$$2''.\ \frac{\delta\check{\mathcal{F}}}{\delta q_n}\Psi_n^* = \frac{\delta\check{\mathcal{F}}}{\delta q_{n+1}}\Psi_{n+1}^*$$

$$3''.\ \text{skew}\left[\frac{\delta\check{\mathcal{F}}}{\delta q_n}\right] = 0.$$

6. Dynamics on Manifolds Open in a Larger Linear Space

The developments in Section 5.4 illustrate some of the difficulties involved in formulating conserving algorithms for Hamiltonian systems on closed Lie groups. Aside from the rather intractable form taken by the symplectic conditions, from a pragmatic standpoint the key difficulty is the lack of an explicit expression for the exponential map. As pointed out in the introduction, if the configuration manifold is open in a larger linear space, this difficulty can be circumvented by replacing the (multiplicative) update dictated by the structure of the configuration manifold with the additive update of the larger linear group. Adopting this strategy, one recovers the conventional setting of conserving algorithms on linear phase spaces.

We illustrate this methodology in the specific setting of a representative example: the dynamics of homogeneous compressible elasticity. First, we provide a brief account of the Hamiltonian structure of this simple mechanical system; we then consider the formulation of symplectic and energy- and momentum-conserving algorithms for this system. Finally, the results are illustrated in sample numerical simulations.

6.1. The Dynamics of Compressible Homogeneous Elasticity

The model under consideration can be viewed as a generalization of classical rigid-body dynamics to incorporate *affine deformations* of a continuum body occupying a reference configuration $\mathcal{B} \subset \mathbb{R}^3$. This motivates the denomination of *pseudo-rigid bodies* coined in Cohen and Muncaster [1984, 1988]. The theory of pseudo-rigid bodies can be derived from classical three-dimensional nonlinear elasticity by constraining the elastic body to homogeneous deformations. A complete treatment of the resulting Hamiltonian systems is given in Lewis and Simo [1989]. The brief summary given below is restricted to those aspects needed for our subsequent algorithmic developments. For simplicity, we assume that the center of mass of the body is a fixed point.

6.1.1. Lagrangian Description: Canonical Hamilton's Equations. The configuration manifold of pseudorigid bodies is the group $Q := Gl^+(3)$ of invertible 3×3 with positive determinant, which is open in the general linear group $L(3)$. (For the incompressible problem the configuration manifold is the group $SL(3)$ of volume- and orientation-preserving matrices which is closed in $L(3)$.) The canonical phase space is the cotangent bundle T^*Q. Tangent and cotangent vectors at a point $F \in Q$ can

be identified with 3×3 matrices in $L(3)$, denoted by V and P, respectively. The identification $T^*Q \approx Q \times L(3)$ via coordinates (F, P), with $F \in Q$ and $P \in L(3)$, is referred to as the material or Lagrangian description of pseudorigid bodies.

The duality pairing between T^*Q and TQ is the standard matrix inner product $\langle P, V\rangle := \mathrm{tr}[P^T V]$. The canonical symplectic two-form on the cotangent bundle T^*Q is defined as

$$\omega(F, P)((\delta F_1, \delta P_1), (\delta F_2, \delta P_2)) := \langle \delta P_2, \delta F_1\rangle - \langle \delta P_1, \delta F_2\rangle. \tag{6.1}$$

Let $W(C)$ denote the stored energy function for the homogeneous material, expressed as a function of the right Cauchy–Green tensor $C := F^T F$, and denote by E the inertia tensor of the continuum body in its reference placement. In the absence of body and surface forces, the Hamiltonian function for homogeneous elasticity forces is

$$H(F, P) := K(P) + W(F^T F), \quad \text{where } K(V) := \frac{1}{2}\langle P, PE^{-1}\rangle \tag{6.2}$$

is the kinetic energy. Denoting by $V := PE^{-1}$ the velocity field associated with the momentum P, the canonical Hamilton's equations (in the Lagrangian description) then take the form

$$\dot{F} = V \quad \text{and} \quad \dot{P} = -2F\nabla W(F^T F). \tag{6.3}$$

6.1.2. Conservation Laws and Momentum Maps. Since the Hamiltonian system under consideration is autonomous, the Hamiltonian flow exactly conserves the total energy in the sense that $\dot{H} = 0$.

Inspection of (6.2) reveals that $H(F, P)$ is left invariant under the action of $SO(3)$, in the sense that $H(QF, QP) = H(F, P)$ for any $Q \in SO(3)$. The conserved quantity induced by this invariance property is the momentum map $\Phi : T^*Q \to \mathbb{R}^3$, given by

$$\Phi(F, P) = \mathrm{rot}\left[PF^T\right], \tag{6.4}$$

and interpreted as the total angular momentum of the system relative to an inertial frame. The additional conservation law is $\dot{\Phi} = \mathbf{0}$.

Of course, the Hamiltonian flow defines a symplectic transformation in phase space that preserves exactly the symplectic two-form defined by (6.1); hence, $\dot{\omega} = \mathbf{0}$ along the flow.

6.2. Conserving Algorithms on $GL^+(3)$

We start our analysis of energy-momentum and symplectic algorithms by considering the following general class of one-step methods:

$$\left.\begin{aligned} F_{n+1} - F_n &= \Delta t\, P_{n+\beta} E^{-1} \\ P_{n+1} - P_n &= \Delta t\, \mathcal{F}(F_{n+1}, F_n) \end{aligned}\right\}, \tag{6.5}$$

where

$$P_{n+\beta} := \beta P_{n+1} + (1 - \beta) P_n. \tag{6.6}$$

Here $\beta \in [0, 1]$ is a parameter defining the algorithm and $\mathscr{F} : L(3) \times L(3) \to L(3)$ is an arbitrary function, left unspecified at this point, and only subject to the usual requirement of consistency with the right-hand side of (6.3). Our objective is to determine the additional restrictions placed on this function by the condition of exact momentum and energy conservation. The analysis given below follows the approach proposed in Simo and Tarnow [1992] in the context of three-dimensional nonlinear elastodynamics.

Result 12 can be applied to this example, yielding the momentum-conservation condition

$$0 = \langle \mathscr{F}(F_{n+1}, F_n), \hat{\xi} F_{n+(1-\beta)} \rangle = \langle \mathscr{F}(F_{n+1}, F_n) F^T_{n+(1-\beta)}, \hat{\xi} \rangle, \tag{6.7}$$

where

$$F_{n+\alpha} := \alpha F_{n+1} + (1 - \alpha) F_n \quad \text{for all } \alpha \in [0, 1], \tag{6.8}$$

for all $\xi \in \mathbb{R}^3$. In view of (6.7), we conclude:

Result 15. *The algorithm (6.5) preserves exactly the momentum map if*

$$\mathscr{F}(F_{n+1}, F_n) = F_{n+\alpha} S(F_{n+1}, F_n) \quad \text{and} \quad \beta = (1 - \alpha), \tag{6.9}$$

for any symmetric matrix $S(F_{n+1}, F_n)$ and any $\alpha \in [0, 1]$.

Observe that momentum-conserving algorithms need not be consistent with the governing equations. Next, we examine the restrictions placed by conservation of energy on the general class of momentum-conserving algorithms identified in the preceding result.

It is well-known that the (implicit) midpoint rule is an exact energy-conserving algorithm in the linear regime. Motivated by this result, we shall restrict our attention to the specific case in which $\alpha = \frac{1}{2}$. Result 13, along with formulas (6.5) and (6.9), implies that for $\alpha = \frac{1}{2}$ energy is conserved if and only if

$$\begin{aligned} W(C_n) - W(C_{n+1}) &= \langle \mathscr{F}(F_{n+1}, F_n), \Omega_{n+(1/2)} \rangle \\ &= \langle F_{n+(1/2)} S(F_{n+1}, F_n), F_{n+1} - F_n \rangle \\ &= \tfrac{1}{2} \langle S(F_{n+1}, F_n), C_{n+1} - C_n \rangle, \end{aligned} \tag{6.10}$$

where $C_{n+1} := F^T_{n+1} F_{n+1}$ and $C_n := F^T_n F_n$. As in the case of three-dimensional elasticity, the preceding condition can be exploited to arrive at the following:

Result 16. *The family of algorithms defined by*

$$\left.\begin{aligned} F_{n+1} - F_n &= \Delta t \; P_{n+(1/2)} E^{-1} \\ P_{n+1} - P_n &= -\Delta t \nabla_F W(C_{n+\gamma}) \;=\; -2\Delta t F_{n+(1/2)} \nabla_C W(C_{n+\gamma}) \end{aligned}\right\}, \tag{6.11}$$

where

$$C_{n+\gamma} := \gamma C_{n+1} + (1 - \gamma) C_n \;=\; \gamma F^T_{n+1} F^T_{n+1} + (1 - \gamma) F^T_n F_n \tag{6.12}$$

and $\gamma \in [0, \frac{1}{2})$ *is determined by the equation*

$$W(C_{n+1}) - W(C_n) = \langle \nabla_C W(C_{n+\gamma}), C_{n+1} - C_n \rangle, \tag{6.13}$$

exactly conserves the total energy (6.2). In addition, the algorithm

$$\left.\begin{aligned} F_{n+1} - F_n &= \Delta t\, P_{n+(1/2)} E^{-1} \\ P_{n+1} - P_n &= -\Delta t\, F_{n+(1/2)} \left(\nabla W_C(C_{n+\gamma}) + \nabla_C W(C_{n+(1-\gamma)}) \right) \end{aligned}\right\} \tag{6.14}$$

conserves exactly energy and momentum and is second-order accurate.

To complete the analysis, it only remains to establish the conditions under which the general class of algorithms defined by (6.5), subject to the momentum-conserving conditions (6.9), is symplectic. To apply Result 14, we first compute the derivatives

$$\left.\begin{aligned} \Psi_n \delta P &= (1-\alpha)\delta P E^{-1} \\ \Psi_{n+1} \delta P &= \alpha \delta P E^{-1} \\ \frac{\partial}{\partial F_n} \mathcal{F}(F_{n+1}, F_n) &= \alpha S(F_{n+1}, F_n) + F_{n+\alpha} \frac{\partial}{\partial F_n} S(F_{n+1}, F_n) \\ \frac{\partial}{\partial F_n} \mathcal{F}(F_{n+1}, F_n) &= (1-\alpha) S(F_{n+1}, F_n) + F_{n+\alpha} \frac{\partial}{\partial F_{n+1}} S(F_{n+1}, F_n) \end{aligned}\right\}. \tag{6.15}$$

Since the derivatives Ψ_n and Ψ_{n+1} are symmetric and $\boldsymbol{H}(\Theta) = \mathbf{1}$ for all Θ, the non-trivial symplectic conditions for the canonical symplectic two-form (6.1) are simply

$$(1-\alpha) \frac{\partial}{\partial F_n} S(F_{n+1}, F_n) = \alpha \frac{\partial}{\partial F_{n+1}} S(F_{n+1}, F_n) = U F_{n+\alpha}^T \tag{6.16}$$

for some symmetric matrix U. The choice

$$\mathcal{F}(F_{n+1}, F_n) = -\nabla_F W(F_{n+\alpha}^T F_{n+\alpha}) \tag{6.17}$$

renders symplectic the exact momentum-conserving algorithms in Result 15 for any $\alpha \in [0, 1]$. In particular, for $\alpha = \frac{1}{2}$ one recovers the well-known symplectic property of the midpoint rule. We remark that for $\alpha \neq \frac{1}{2}$ this one-parameter family of simplectic algorithms is only first-order accurate and conditionally stable; see Simo, Tarnow, and Wong [1992]. Note that the algorithms (6.11) and (6.14) do *not* satisfy (6.16) and hence are not symplectic.

6.3. Delay Plots for Conserving Algorithms

The momentum-conserving symplectic algorithms determined by (6.5) and (6.17) do *not* conserve energy. However, the energy along the algorithmic trajectory remains bounded throughout very long simulations. (It is popularly believed that this is a common characteristic of symplectic algorithms.) In fact, the approximate energy appears to be quasi-periodic. We provide below visualizations of the evolution of the total energy for sample initial conditions using delay-reconstruction techniques. Attractor reconstruction from scalar data is common in several areas of dynamical systems. (See, for example, Packard et al. [1980] for a discussion of reconstruction

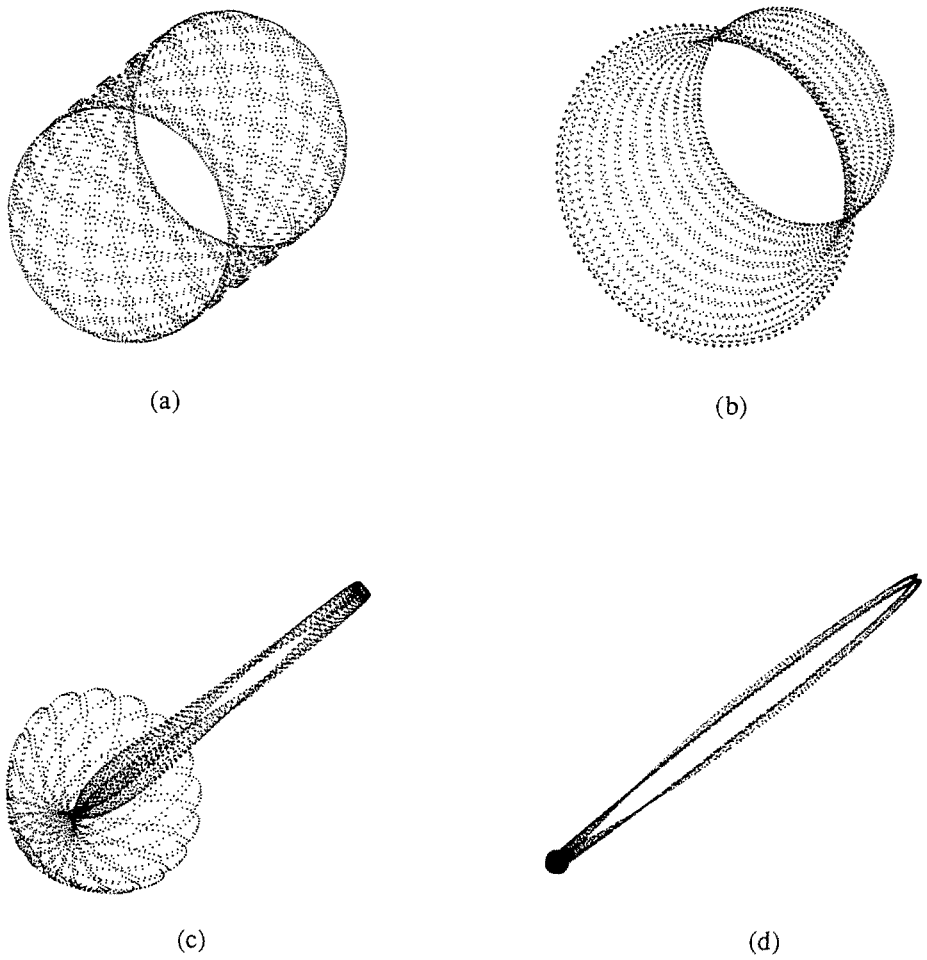

Fig. 3. Energy delay plots. Time-step: .005; delay: 3; initial configuration: 1; angular momentum: (a) .4, (b) 2.0, (c) 6.0, (d) 10.0; energy variation: (a) $4.0 \cdot 10^{-8}$, (b) $1.8 \cdot 10^{-5}$, (c) $2.3 \cdot 10^{-3}$, (d) $1.6 \cdot 10^{-1}$.

techniques.) We employ here an extremely simple version of these techniques: We numerically compute a time series $\{(F_n, P_n)\}$ with initial conditions (F_0, P_0); we map this sequence of elements in $GL(3) \times L(3)$ to the real-valued sequence $\{H_n\}$ consisting of the total energy at each time-step; finally, we plot the sequence $\{(H_n, H_{n+N}, H_{n+2N})\}$ of three vectors determined by an integer delay parameter N.

All delay plots that we have made to date using the symplectic algorithm determined by (6.5) and (6.17) result in tori or deformed tori; we provide several samples of such plots below. The plots in Fig. 3 for initial conditions consisting of a sphere rotating with a relatively low angular velocity show only slightly deformed tori, while increasing angular velocity leads to increasingly dramatic deformations of the tori. Figure 4 shows integrations of two of the initial conditions used in Fig. 3, using the

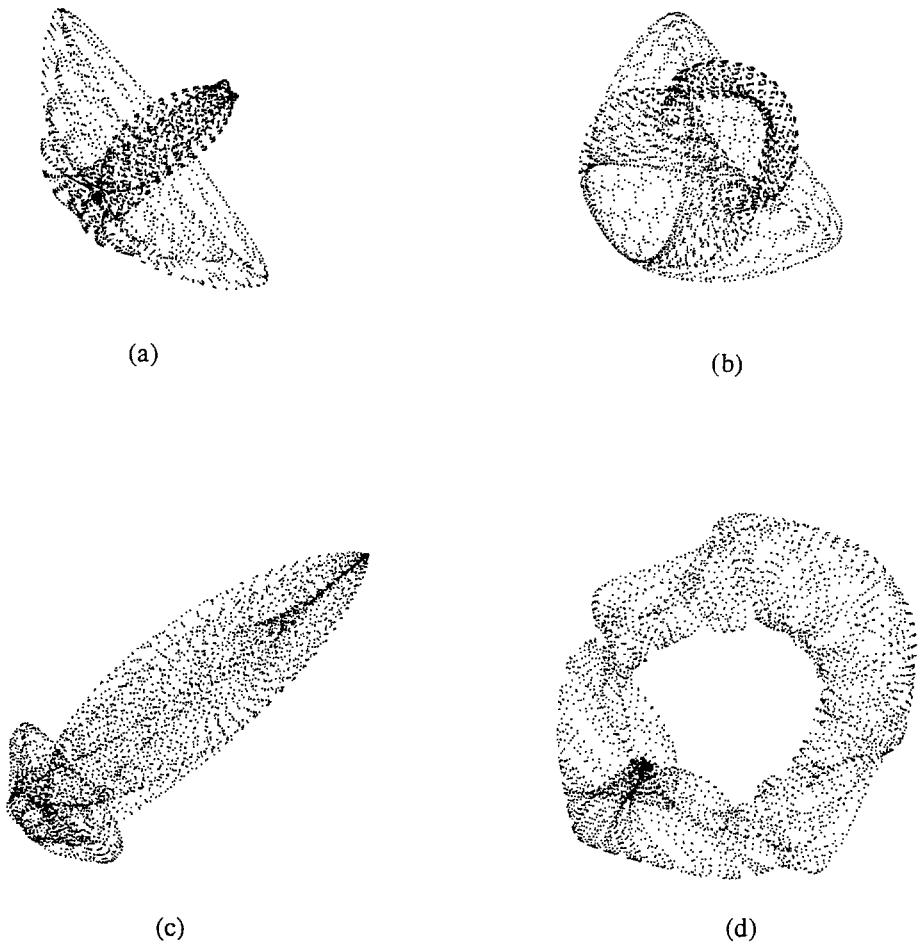

Fig. 4. Energy delay plots. Time-step: .05; delay: (a, c) 3, (b, d) 5; initial configuration: 1; angular momentum: (a, b) 6.0, (c, d) 10.0; energy variation: (a, b) $3.9 \cdot 10^{-1}$, (c, d) 6.2.

time-step $\Delta t = 0.05$, rather than the time-step $\Delta t = 0.005$ used in Fig. 3, and two choices of delay. Note: While increasing the time-step from 0.005 to 0.05 yields a substantial change in the size of the figures, it does not (in our opinion) result in a significant change in the qualitative structure of the figures. The symplectic algorithm determined by (6.17) and the energy-conserving algorithms (6.11) and (6.14) all yield slightly deformed tori in delay plots of the norm $\|F_n - \mathbf{1}\|$ of the displacement. Figures 5(c) and 5(d) show representative plots; 5(c) is computed using the energy-conserving algorithm determined by (6.13), while 5(d) is computed using (6.5) and (6.17). All of the integrations except that plotted in Fig. 5(c) model a Mooney–Rivlin material with parameters $\lambda = 2000$, $\mu = 6$, and $\beta = 0.5$; in 5(c) a Saint–Venant–Kirchhoff material with parameters $\lambda = 2000$ and $\mu = 6$ is used.

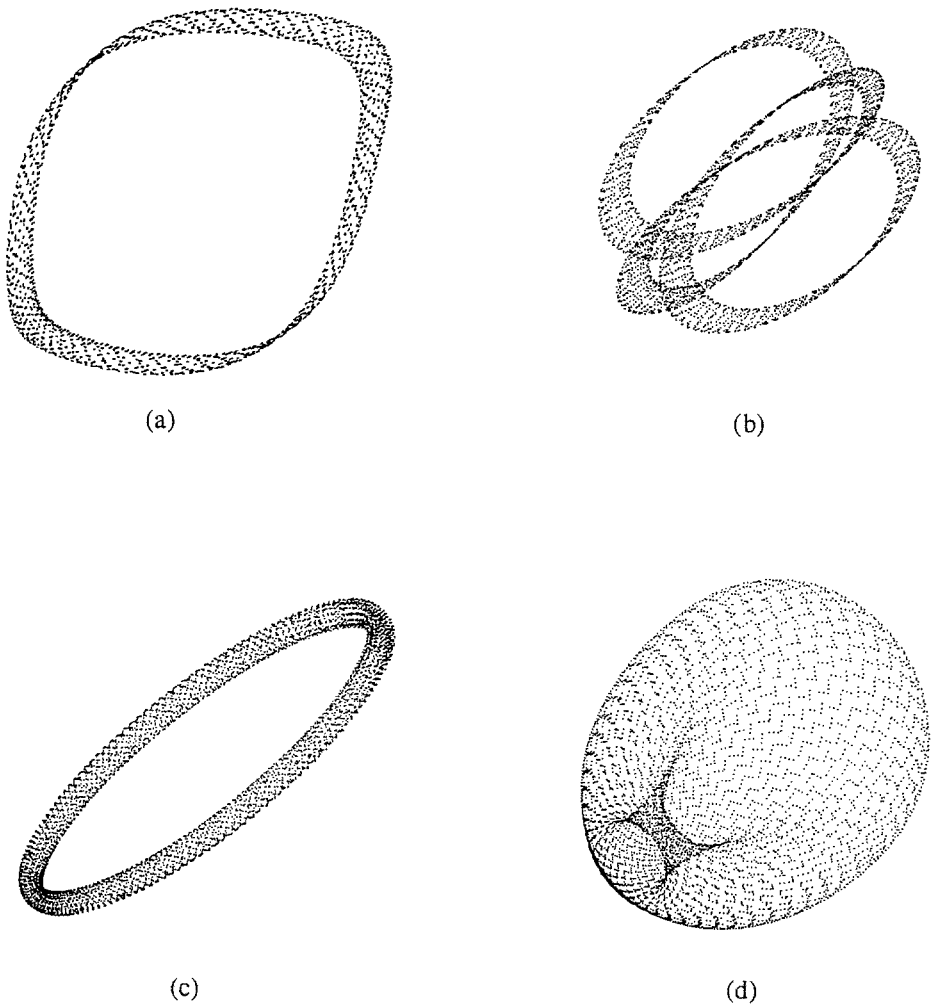

Fig. 5. Energy and displacement delay plots. Time-step: (a) .005, (b, d) .05, (c) .001; delay: (a, c) 3, (b, d) 5; initial configuration: (a, b, c) ((1.01, .01, 0), (.01, 1.01, 0), (0, 0, .99)), (d) 1; angular momentum: (a, b, c) 0, (d) 10.0; energy variation: (a) 1.6, (b) $2.0 \cdot 10^{-2}$; displacement variation (c) $3.1 \cdot 10^{-4}$, (d) 32.1.

Acknowledgments

We are indebted to Francisco Armero and Nils Tarnow for many discussions on the topics of this paper. Support for this research was provided by NSF Grant DMS-9122708 and FRC Grant 503128-09523 through U.C. Santa Cruz and AFOSR Contract No. 2-DJA-826 through Stanford University. This support is gratefully acknowledged.

Appendix A: Source Code for the Integration of the Unreduced Euler Equations on $SO(3)$ and Tracking of the Poisson Error

We include here the *Mathematica* code used to generate the plots of the Poisson error given in Section 3.3. Our motivation for this is two-fold: first, to allow the reader to experiment with different initial conditions and different scalings of the Cayley transformation; second, to demonstrate that the energy- and momentum-conserving algorithms discussed in Section 2 are actually quite simple to implement.

We first define the required maps and functions: `skew` takes a three-vector to a skew-symmetric matrix; `rot` takes a three-by-three matrix `M` to the three-vector such that `skew[rot[M]]` is the skew-symmetric part of M. `cayley` is, of course, the Cayley transformation (2.5) taking a three-vector to a rotation matrix. `kapcay`, `kapexp`, and `kapsym` are the scaling functions associated to the Cayley, exponential, and symplectic maps.

```
id = IdentityMatrix[3]
norm = Sqrt[#.#]&
skew = {{0, -#[[3]], #[[2]]},
        {#[[3]], 0, -#[[1]]},
        {-#[[2]], #[[1]], 0}}&
rot = {-#[[2,3]], #[[1,3]], -#[[1,2]]}/2&[# - Transpose[#]]&
cayley = (id + #).Inverse[id - #]&[skew[#/2]]&
kapcay = 1&
kapexp = (Tan[#]/#)&[norm[#]/2]&
kapsym = If[TrueQ[# > 1], (Print["\nTheta is too big!\n"]; 2),
           2/(1 + Sqrt[1 - #^2])]&[norm[#]]&
```

The function `step` performs a single step of the integration using the algorithm (3.3), where $\mathbf{T} : \mathbb{R}^3 \to SO(3)$ is a scaled Cayley transformation with scaling function `kappa`. The integration "driver" `int`, which is based on the Runge–Kutta driver given in Maeder [1991], integrates from the initial configuration-momentum pair (`lambda`, `pi`) for a time period of length `t`, using fixed time-steps of size `dt`. The matrix `j` is the body inertia tensor; `options` can include any (or none) of the optional arguments of the *Mathematica* function `FindRoot`.

```
step[{lambda_, theta_}, kappa_, pi_, j_, dt_, options_] :=
   Block[{x, y, z},
      {lambda.cayley[kappa[#] #], #}&[#1/.FindRoot[
         (id + kappa[#1]/2 skew[#1]).j.#1 ==
            dt Transpose[lambda].pi, ##2, options]&@@
         Prepend[Transpose[{#, theta}], #]&[{x, y, z}]]]

int[lambda_, kappa_, pi_, j_, t_, dt_, options_] :=
   NestList[step[#, kappa, pi, j, dt, options]&,
      N[{lambda, dt Inverse[j].Transpose[lambda].pi}],
      Round[t/dt]]
```

The Poisson error is computed according to the formula (3.28) using (3.23) and (3.29). The function pstep computes the Poisson error at a single time-step, while poiserr determines the Poisson error over a series of time-steps. The function muexp is the parameter μ, with general expression (3.23), associated with the exponential map; the expressions $\mu = 0$ (respectively, $\mu = 2$) associated to the Cayley (respectively, symplectic) maps are sufficiently simple that they are explicitly given in the Switch statement.

```
muexp = (3 - 1l Cos[#])(# - Sin[#])/((Cos[#] - 1) #)&[norm[#]]&


pstep[sigma_, {lambda_, theta_}, kappa_, pihat_, j_, dt_] :=
   With[{kap = kappa[theta]},
      Fold[#2[#1]&, Switch[kappa, kapcay, 0,
            kapexp, muexp[theta], kapsym, 2],
         {id/kap - skew[theta]/2 +
            kap (1 - #)/4 Outer[Times, theta, theta]&,
         (2/dt lambda.#.j.Transpose[lambda] + pihat).
            (id + kap/2 skew[lambda.theta])&,
         sigma + 4/Det[#] #.rot[(id + pihat.skew[sigma]).
            (# - pihat)]&}]]


poiserr[pairs_, kappa_, pi_, j_, dt_] :=
   FoldList[pstep[#1, #2, kappa, skew[pi], j, dt]&,
   {0, 0, 0}, pairs]
```

The functions plotScalar and showtop can be used to compute and display trajectories, their energy, and the magnitude of the Poisson error. plotScalar takes as its arguments a text string label which serves as a label for a two-dimensional plot, a real-valued function fcn which is to be plotted, and a list data of data points to which fcn is to be applied. showtop takes as input initial conditions (lambda, pi), a scaling function kappa, a three-vector jdiag giving the diagonal entries of the body inertia tensor (for convenience, we assume that the inertia tensor is diagonal—this can be easily modified to accept a general symmetric matrix), an overall time range t and incremental time-step dt, and a (possibly trivial) list of options for the *Mathematica* command FindRoot used in the integration. showtop performs the specified integration, creates a three-dimensional plot tracing the positions of the tips of the unit coordinate axes as rotated by the attitude matrices, and, finally, plots the energy of the system and the magnitude of the Poisson error.

```
plotScalar[label_, fcn_, data_] :=
   ListPlot[#1, PlotJoined ->True, PlotLabel-> #2]&@@{#,
      StringJoin[label, "\nmaximum variation (max - min):\n",
         ToString[InputForm[Max[#] - Min[#]]]]}&[fcn/@ data]
```

```
showtop[lambda_, kappa_, pi_, jdiag_, t_, dt_, options_] :=
   Module[{j = DiagonalMatrix[jdiag],
         jinv = DiagonalMatrix[1/jdiag],
         outlist = int[lambda, kappa, pi, j, t, dt, options],
         attitude},
      attitude = First/@outlist;
      Show[Graphics3D[{RGBColor@@#, Line[attitude.#]}&/@id]];
      plotScalar["energy", ((#.jinv.#/2)&[Transpose[#].pi])&,
         attitude];
      plotScalar["Poisson error", norm[#]&,
         poiserr[outlist, kappa, pi, j, dt]]]
```

Appendix B: Derivation of Energy Conservation and Symplectic Conditions for Algorithms on General Lie Groups

The proof of Results 3 and 10, giving conditions for the conservation of energy for Euler and general Hamiltonian systems, proceeds as follows. We shall prove the general case, which can then be specialized to the unreduced Euler equations by setting the potential and the algorithmic "force" equal to zero. For convenience, let $\tilde{\mathcal{F}}_n := \mathrm{Ad}^*_{q_n} \mathcal{F}(q_n, \Theta)$. Equation (5.43) implies that

$$\Pi_n = \mathrm{Ad}_{q_n} \pi_n = \mathrm{Ad}_{q_n}(\pi_{n+1} - \Delta t \mathcal{F}(q_n, \Theta)) = \mathrm{Ad}^*_{\tau}(\Theta)^{-1} \Pi_{n+1} - \Delta t \tilde{\mathcal{F}}_n. \quad (6.18)$$

Solving

$$2\mathbf{m}\Omega_{n+(1/2)} = \Pi_{n+1} + \Pi_n = \mathcal{S}_n \Pi_{n+1} - \Delta t \tilde{\mathcal{F}}_n, \quad (6.19)$$

where $\mathcal{S}_n = \mathbf{1} + \mathrm{Ad}^*_{\tau(\Theta)^{-1}}$, for Π_{n+1} yields

$$\Pi_{n+1} = \mathcal{S}_n^{-1} \left(2\dot{\mathbf{m}}\Omega_{n+(1/2)} + \Delta t \tilde{\mathcal{F}}_n \right). \quad (6.20)$$

Combining (6.18) and (6.20) yields

$$\Pi_{n+1} - \Pi_n = 2\mathcal{S}_n^{-1} \left(\left(\mathbf{1} - \mathrm{Ad}^*_{\tau(\Theta)^{-1}} \right) \mathbf{m}\Omega_{n+(1/2)} + \Delta t \tilde{\mathcal{F}}_n \right). \quad (6.21)$$

Thus energy is conserved if

$$\begin{aligned} & V(q_n) - V(q_{n+1}) \\ &= \frac{1}{2} \|\Pi_{n+1}\|^2_{\mathfrak{g}^*} - \frac{1}{2} \|\Pi_n\|^2_{\mathfrak{g}^*} \\ &= \langle \Pi_{n+1} - \Pi_n, \Omega_{n+(1/2)} \rangle \\ &= 2 \left\langle \left(\mathbf{1} - \mathrm{Ad}^*_{\tau(\Theta)^{-1}} \right) \mathbf{m}\Omega_{n+(1/2)} + \Delta t \tilde{\mathcal{F}}_n, \left(\mathbf{1} + \mathrm{Ad}_{\tau(\Theta)^{-1}} \right)^{-1} \Omega_{n+(1/2)} \right\rangle. \end{aligned} \quad (6.22)$$

The general energy conservation condition (6.22) implies the Euler equation condition (5.26). The condition $\mathrm{Ad}_{\tau(\Theta)}\Omega_{n+(1/2)} = \Omega_{n+(1/2)}$ implies that

$$\langle \nu, \Omega_{n+(1/2)} \rangle = \langle \mathcal{I}_n^{-1}\nu, \mathbf{1} + \mathrm{Ad}_{\tau(\Theta)^{-1}} \rangle = 2\langle \mathcal{I}_n^{-1}\nu, \Omega_{n+(1/2)} \rangle \tag{6.23}$$

for any $\nu \in \mathcal{G}^*$. Thus (6.22) simplifies to (5.49) (respectively, (5.25)) if

$$\mathrm{Ad}_{\tau(\Theta)}\Omega_{n+(1/2)} = \Omega_{n+(1/2)}.$$

The derivation of the expression for the Poisson error for the unreduced Euler equations proceeds as follows. The linearized equations associated with equations (5.23) are

$$\left.\begin{aligned} \delta q_{n+1} &= \delta q_n + \mathrm{Ad}^*_{q_{n+1}} H(\Theta)\delta\Theta \\ \delta \pi_{n+1} &= \delta \pi_n \\ \delta\Theta &= \frac{\Delta t}{2}\mathbf{m}^{-1}\left(\mathrm{Ad}^*_{q_{n+1}}\left(\mathrm{ad}^*_{\delta q_{n+1}}\pi_{n+1} + \delta\pi_{n+1}\right) + \mathrm{Ad}^*_{q_n}\left(\mathrm{ad}^*_{\delta q_n}\pi_n + \delta\pi_n\right)\right) \end{aligned}\right\}. \tag{6.24}$$

Equations (6.24) can be written in the form

$$\begin{pmatrix} \mathbf{1} + B_{n+1}\alpha & B_{n+1} \\ \mathbf{0} & \mathbf{1} \end{pmatrix}\begin{pmatrix} \delta q_{n+1} \\ \delta \pi_{n+1} \end{pmatrix} = \begin{pmatrix} \mathbf{1} + B_n\alpha & B_n \\ \mathbf{0} & \mathbf{1} \end{pmatrix}\begin{pmatrix} \delta q_n \\ \delta \pi_n \end{pmatrix}, \tag{6.25}$$

where $B_n := M\ \mathrm{Ad}^*_{q_n}$ and $B_{n+1} := -M\mathrm{Ad}^*_{q_{n+1}}$, for

$$M := \frac{\Delta t}{2}\mathrm{Ad}_{q_{n+1}} H(\Theta)\mathbf{m}^{-1}. \tag{6.26}$$

Solving (6.25) for $(\delta q_{n+1}, \delta \pi_{n+1})$ yields (5.29), where

$$\begin{aligned} C_n &:= (\mathbf{1} + B_{n+1}\alpha)^{-1}(B_n - B_{n+1}) \\ &= \mathrm{Ad}_{q_{n+1}}\left(\frac{2}{\Delta t}\mathbf{1} - H(\Theta)\mathbf{m}^{-1}\mathrm{ad}^*\Pi_{n+1}\right)^{-1} H(\Theta)\mathbf{m}^{-1}\left(\mathrm{Ad}^*_{q_n} + \mathrm{Ad}^*_{q_{n+1}}\right), \end{aligned} \tag{6.27}$$

since

$$\mathrm{Ad}^*_{q_{n+1}}\ \mathrm{ad}^*\pi\ \mathrm{Ad}_{q_{n+1}} = \mathrm{ad}^*(\mathrm{Ad}^*_{q_{n+1}}\pi) = \mathrm{ad}^*\Pi_{n+1}. \tag{6.28}$$

Using (3.1) and the identity (3.10), we see that

$$\begin{pmatrix} \mathbf{0} & -\mathbf{1} \\ \mathbf{1} & \alpha \end{pmatrix} = \begin{pmatrix} \mathbf{1} + C_n\alpha & C_n \\ \mathbf{0} & \mathbf{1} \end{pmatrix}\begin{pmatrix} \mathbf{0} & -\mathbf{1} \\ \mathbf{1} & \alpha \end{pmatrix}\begin{pmatrix} \mathbf{1} + C_n\alpha & C_n \\ 0 & \mathbf{1} \end{pmatrix}^* \tag{6.29}$$

if and only if $\mathcal{P}_n = \mathrm{skew}[C_n(2\ \mathbf{1} - \alpha C_n^*)] = 0$. If C_n is invertible, the map is symplectic if and only if

$$2\ \mathrm{skew}\left[C_n^{-1}\right] = -\alpha. \tag{6.30}$$

Condition (6.30) can be simplified as follows: $\mathcal{S}_n$ and $\mathrm{Ad}^*_{q_{n+1}}$ are invertible, hence (6.30) is satisfied if and only if

$$\begin{aligned} 0 &= \mathcal{S}_n \mathrm{Ad}^*_{q_{n+1}} \operatorname{skew}\left[2C_n^{-1} + \alpha\right] \mathrm{Ad}_{q_{n+1}} \mathcal{S}_n^T \\ &= \mathcal{S}_n \operatorname{skew}\left[2\mathcal{S}_n^{-1}\left(\frac{2}{\Delta t}\mathbf{m}\boldsymbol{H}(\Theta)^{-1} - \mathrm{ad}^*\Pi_{n+1}\right) + \mathrm{ad}^*\Pi_{n+1}\right]\mathcal{S}_n^T \\ &= \operatorname{skew}\left[\frac{4}{\Delta}\mathbf{m}\boldsymbol{H}(\Theta)^{-1}\mathcal{S}_n^* + (2\,\mathbf{1} - \mathcal{S}_n)\mathrm{ad}^*\Pi_{n+1}\mathcal{S}_n^*\right]. \end{aligned} \tag{6.31}$$

Equation (6.31) can be further simplified using the identity

$$\begin{aligned} \operatorname{skew}\left[(2\,\mathbf{1} - \mathcal{S}_n)\mathrm{ad}^*\Pi_{n+1}\mathcal{S}_n^*\right] &= \operatorname{skew}\left[\left(\mathbf{1} - \mathrm{Ad}^*_{\tau(\Theta)^{-1}}\right)\mathrm{ad}^*\Pi_{n+1}\left(\mathbf{1} + \mathrm{Ad}_{\tau(\Theta)^{-1}}\right)\right] \\ &= \mathrm{ad}^*\left(\Pi_n - \Pi_{n+1}\right) \end{aligned} \tag{6.32}$$

and equation (6.21) to obtain the symplectic conditions (5.31) and (5.33).

We shall now derive Result 14, which specifies the conditions under which the map (5.43) is symplectic. This derivation is analogous to that given in Section 2. We first consider the linearized equations. If we define

$$\left.\begin{aligned} A_n &:= \Delta t\; G_n \Psi_n \mathrm{Ad}^*_{q_n} & A_{n+1} &:= -\Delta t\; G_n \Psi_{n+1} \mathrm{Ad}^*_{q_{n+1}} \\ B_n &:= \mathrm{Ad}_{q_{n+1}} \boldsymbol{H}(\Theta) \Psi_n \mathrm{Ad}^*_{q_n} & B_{n+1} &:= -\mathrm{Ad}_{q_{n+1}} \boldsymbol{H}(\Theta) \Psi_{n+1} \mathrm{Ad}^*_{q_{n+1}} \\ \alpha_n &:= \mathrm{ad}^* \pi_n & \alpha_{n+1} &:= \mathrm{ad}^* \pi_{n+1} \end{aligned}\right\}, \tag{6.33}$$

then the linearization of (5.41) has the form

$$(\delta q_{n+1}, \delta \pi_{n+1}) = \tilde{L}_{n+1}^{-1} \tilde{L}_n (\delta q_n, \delta \pi_n), \tag{6.34}$$

where

$$\tilde{L}_n := \begin{pmatrix} \mathbf{1} + B_n \alpha_n & B_n \\ A_n \alpha_n + \Delta t\; F_n & \mathbf{1} + A_n \end{pmatrix} \tag{6.35}$$

and

$$\tilde{L}_{n+1} := \begin{pmatrix} \mathbf{1} + B_{n+1} \alpha_{n+1} & B_{n+1} \\ A_{n+1} \alpha_{n+1} & \mathbf{1} + A_{n+1} \end{pmatrix}. \tag{6.36}$$

As we did for the free rigid body in Section 3.1, we express the test for symplecticity in the form

$$\tilde{L}_n \begin{pmatrix} \mathbf{0} & -\mathbf{1} \\ \mathbf{1} & \alpha_n \end{pmatrix} \tilde{L}_n^* = \tilde{L}_{n+1} \begin{pmatrix} \mathbf{0} & -\mathbf{1} \\ \mathbf{1} & \alpha_{n+1} \end{pmatrix} \tilde{L}_{n+1}^*. \tag{6.37}$$

A straightforward calculation shows that

$$\tilde{L}_n \begin{pmatrix} \mathbf{0} & -\mathbf{1} \\ \mathbf{1} & \alpha_n \end{pmatrix} \tilde{L}_n^* = \begin{pmatrix} \operatorname{skew}\left[B_n\left(2\,\mathbf{1} - \alpha_n B_n^*\right)\right] & -\mathbf{1} - (\mathbf{1} + B_n \alpha_n) A_n^* + \Delta t\; B_n F_n^* \\ \mathbf{1} + A_n\left(\mathbf{1} - \alpha_n B_n^*\right) - \Delta t\, F_n B_n^* & \alpha_{n+1} - A_n \alpha_n A_n^* - \Delta t\; k(q_n, \Theta) \end{pmatrix}, \tag{6.38}$$

where

$$k(q_n, \Theta) := \mathrm{ad}^*\mathcal{F}(q_n, \Theta) + 2\ \mathrm{skew}\left[F_n\left(\mathbf{1} + A_n^*\right)\right], \tag{6.39}$$

and

$$L_{n+1}\begin{pmatrix}\mathbf{0} & -\mathbf{1}\\ \mathbf{1} & \alpha_{n+1}\end{pmatrix}L_{n+1}^* = \begin{pmatrix}\mathrm{skew}[B_{n+1}(2\ \mathbf{1} - \alpha_{n+1}B_{n+1}^*)] & -\mathbf{1} - (\mathbf{1} + B_{n+1}\alpha_{n+1})A_{n+1}^*\\ \mathbf{1} + A_{n+1}(\mathbf{1} - \alpha_{n+1}B_{n+1}^*) & \alpha_{n+1} - A_{n+1}\alpha_{n+1}A_{n+1}^*\end{pmatrix}. \tag{6.40}$$

Thus the algorithm (5.41) is symplectic if:

1. $B_{n+1}\alpha_{n+1}B_{n+1}^* - B_n\alpha_nB_n^* = 2\ \mathrm{skew}[B_{n+1} - B_n]$
2. $A_{n+1}\left(\alpha_{n+1}B_{n+1}^* - \mathbf{1}\right) - A_n\left(\alpha_nB_n^* - \mathbf{1}\right) = \Delta t\ F_nB_n^*$
3. $A_{n+1}\alpha_{n+1}A_{n+1}^* - A_n\alpha_nA_n^* = \Delta t\ k(q_n, \Theta)$.

We shall now rearrange and simplify these conditions to obtain the conditions given in Result 14. The first condition can be regrouped using the relations

$$\begin{aligned}&B_{n+1}\alpha_{n+1}B_{n+1}^* - B_n\alpha_nB_n^*\\ &\quad = \mathrm{Ad}_{q_{n+1}}\boldsymbol{H}(\Theta)\left(\Psi_{n+1}\mathrm{ad}^*\Pi_{n+1}\Psi_{n+1}^* - \Psi_n\mathrm{ad}^*\Pi_n\Psi_n^*\right)\boldsymbol{H}(\Theta)^*\mathrm{Ad}_{q_{n+1}}^*\end{aligned} \tag{6.41}$$

and

$$\begin{aligned}&\mathrm{skew}[B_{n+1} - B_n]\\ &\quad = \mathrm{Ad}_{q_{n+1}}\boldsymbol{H}(\Theta)\ \mathrm{skew}\left[(\Psi_{n+1} + \Psi_n\mathrm{Ad}_{\tau(\Theta)^{-1}}^*)\boldsymbol{H}(\Theta)^{-T}\right]\boldsymbol{H}(\Theta)^*\mathrm{Ad}_{q_{n+1}}^*\end{aligned} \tag{6.42}$$

to show that condition 1 holds if and only if

$$2\ \mathrm{skew}\left[\boldsymbol{H}(\Theta)^{-1}\left(\Psi_{n+1}^* + \mathrm{Ad}_{\tau(\Theta)^{-1}}\Psi_n^*\right)\right] = \Psi_{n+1}\mathrm{ad}^*\Pi_{n+1}\Psi_{n+1}^* - \Psi_n\mathrm{ad}^*\Pi_n\Psi_n^*. \tag{6.43}$$

The second condition is simplified by noting that if condition 1 is satisfied, then

$$\begin{aligned}&A_n\left(\mathbf{1} - \alpha_nB_n^*\right) - A_{n+1}\left(\mathbf{1} - \alpha_{n+1}B_{n+1}^*\right)\\ &\quad = \Delta t\ G_n\Big(\left(\Psi_{n+1} + \Psi_n\mathrm{Ad}_{\tau(\Theta)^{-1}}^*\right)\boldsymbol{H}(\Theta)^{-T}\\ &\qquad + \Psi_{n+1}\mathrm{ad}^*\Pi_{n+1}\Psi_{n+1}^*\\ &\qquad - \Psi_n\mathrm{ad}^*\Pi_n\Psi_n^*\Big)\boldsymbol{H}(\Theta)^*\mathrm{Ad}_{q_{n+1}}^*\\ &\quad = \Delta t\ G_n\boldsymbol{H}(\Theta)^{-1}\left(\Psi_{n+1}^* + \mathrm{Ad}_{\tau(\Theta)^{-1}}\Psi_n^*\right)\boldsymbol{H}(\Theta)^*\mathrm{Ad}_{q_{n+1}}^*.\end{aligned} \tag{6.44}$$

Thus if condition 1 holds, then condition 2 is equivalent to

$$G_n\boldsymbol{H}(\Theta)^{-1}\left(\Psi_{n+1}^* + \mathrm{Ad}_{\tau(\Theta)^{-1}}\Psi_n^*\right) = F_n\mathrm{Ad}_{q_n}^*\Psi_n^*. \tag{6.45}$$

If the first two conditions hold, then condition 3 can be rewritten using

$$\begin{aligned} A_n\alpha_{n+1}A_{n+1}^* - A_n\alpha_n A_n^* &= \Delta t^2\, G_n\left(\Psi_{n+1}\mathrm{ad}^*\Pi_{n+1}\Psi_{n+1}^* - \Psi_n\mathrm{ad}^*\Pi_n\Psi_n^*\right)G_n^* \\ &= 2\Delta t^2\ \mathrm{skew}\left[G_n H(\Theta)^{-1}\left(\Psi_{n+1}^* + \mathrm{Ad}_{\tau(\Theta)^{-1}}\Psi_n^*\right)G_n^*\right] \\ &= 2\Delta t^2\ \mathrm{skew}\left[F_n\mathrm{Ad}^*_{q_n^{-1}}\Psi_n^* G_n^*\right] \\ &= 2\Delta t\ \mathrm{skew}\left[F_n A_n^*\right] \\ &= \Delta t\ \left(k(q_n,\Theta) - \mathrm{ad}^*\mathcal{F} - 2\ \mathrm{skew}[F_n]\right). \end{aligned} \tag{6.46}$$

Thus the third condition holds if conditions 1 and 2 hold and $\mathrm{ad}^*\mathcal{F} = -2\ \mathrm{skew}[F_n]$.

References

R. Abraham and J. E. Marsden [1978] *Foundations of Mechanics*, 2nd ed., Addison-Wesley, Reading, MA.

V. I. Arnold [1988] *Mathematical Methods of Classical Mechanics*, Springer-Verlag, New York.

M. Austin, P. S. Krishnaprasad, and L. S. Wan [1992] "Almost Lie-Poisson Integrators for the Rigid Body," preprint.

A. Bayliss and E. Isaacson [1975] "How to Make Your Algorithm Conservative," *American Mathematical Society*, A594–A595.

P. J. Channell [1983] *Symplectic Integration Algorithms*, Los Alamos National Laboratory Internal Report AT-6:ATN-83-9.

P. J. Channell and J. C. Scovel [1989] "Symplectic Integration of Hamiltonian Systems," preprint.

H. Cohen and R. G. Muncaster [1984] "The Dynamics of Psuedo-Rigid Bodies: General Structure and Exact Solutions," *J. Elasticity*, **14**, 127–154.

H. Cohen and R. G. Muncaster [1988] *The Theory of Pseudo-Rigid Bodies*, Springer-Verlag, New York.

Y. Coquete-Bruhat and C. DeWitt-Morette [1982] *Analysis, Manifolds and Physics*, North-Holland, Amsterdam.

M. L. Curtis [1984] *Matrix Groups*, Springer-Verlag, Berlin.

R. de Vogelaere [1956] "Methods of Integration Which Preserve the Contact Transformation Property of Hamiltonian Equations," Department of Mathematics, University of Notre Dame, Report 4.

Feng Kan [1986] "Difference Schemes for Hamiltonian Formalism and Symplectic Geometry," *J. Computational Mathematics*, **4**, 279–289.

Feng Kan and M. Qin [1987] *The Symplectic Methods for the Computation of Hamiltonian Equations*, Springer Lect. Notes Math. **1297**, 1–31, Springer-Verlag, Berlin.

H. Goldstein [1982] *Classical Mechanics*, Addison-Wesley, Reading, MA.

D. Greenspan [1984] "Conservative Numerical Methods for $\dot{x} = f(x)$," *J. Computational Physics*, **56**, 28–41.

R. A. Labudde and D. Greenspan [1976a] "Energy and Momentum Conserving Methods of Arbitrary Order for the Numerical Integration of Equations of Motion. Part I," *Numerische Mathematik*, **25**, 323–346.

R. A. Labudde and D. Greenspan [1976b] "Energy and Momentum Conserving Methods of Arbitrary Order for the Numerical Integration of Equations of Motion. Part II," *Numerische Mathematik*, **26**, 1–16.

F. M. Lasagni [1988] "Canonical Runge–Kutta methods," *ZAMP*, **39**, 952–953.

D. Lewis and J. C. Simo [1990] "Nonlinear Stability of Pseudo-Rigid Bodies," *Proceedings of the Royal Society of London A*, **427**, 281–319.

R. Maeder [1991] *Programming in Mathematica*, Addison-Wesley, Redwood City, CA.
A. Marciniak [1984] "Energy Conserving, Arbitrary Order Numerical Solutions of the N-body Problem," *Numerische Mathemathik*, **45**, 207–218.
K. W. Morton [1977] "Initial Value Problems by Finite and Other Methods," in *The State of the Art in Numerical Analysis*, D. A. H. Jacobs, Ed., pp. 699–756, Academic Press, London.
J. Moser and A. P. Veselov [1991] "Discrete versions of some classical integrable systems and factorization of matrix polynomials," *Comm. Math. Phys.*, **139**, 217–243.
N. H. Packard, J. P. Crutchfield, J. D. Farmer, and R. S. Shaw [1980] "Geometry from a Time Series," *Physical Review Letters*, **45**, No. 9, 712–716.
D. I. Pullin and P. G. Saffman [1991] "Long-time Symplectic Integration: The Example of Four-Vortex Motion," *Proceedings of the Royal Society of London A*, **432**, 481–494.
R. D. Richtmyer and K. W. Morton [1967] *Difference Methods for Initial Value Problems*, 2nd ed., Wiley-Interscience, New York.
J. M. Sanz-Serna [1988] "Runge–Kutta Schemes for Hamiltonian Systems," *BIT*, **28**, 877–883.
J. M. Sanz-Serna [1992] "The Numerical Integration of Hamiltonian Systems," Proceedings of the Conference on Computational Differential Equations, Imperial College, London, 3–7 July 1989, in press.
C. Scovel [1991] "Symplectic Numerical Integration of Hamiltonian Systems," in *The Geometry of Hamiltonian Systems*, Proceedings of the Workshop held June 5–15, 1989, Tudor Ratiu, Ed., Springer-Verlag, New York, pp. 463–496.
J. C. Simo and K. K. Wong [1991] "Unconditionally Stable Algorithms for Rigid Body Dynamics That Exactly Preserve Energy and Momentum," *International J. Numerical Methods in Engineering*, **31**, 19–52.
J. C. Simo, M. S. Rifai, and D. D. Fox [1991] "On a Stress Resultant Geometrically Exact Shell Model. Part VI: Conserving Algorithms for Nonlinear Dynamics," *International J. Numerical Methods in Engineering*, **34**, 117–164.
J.C. Simo and N. Tarnow [1992] "The Discrete Energy-Momentum Method. Conserving Algorithms for Nonlinear Elastodynamics," *Zeitschrift für Angewandte Mathematik und Physik*, **43**, 757–792.
J. C. Simo, N. Tarnow, and K. Wong [1992] "Exact Energy-Momentum Conserving Algorithms and Symplectic Schemes for Nonlinear Dynamics," *Computer Methods in Applied Mechanics and Engineering*, **100**, 63–116.
J. C. Simo and R. L. Taylor [1991] "Finite Elasticity in Principal Stretches: Formulation and Augmented Lagrangian Algorithms," *Computer Methods in Applied Mechanics and Engineering*, **85**, 273–310.
S. S. Smale [1970a] "Topology and Mechanics, Part I," *Inventiones Mathematicae*, **10**, 161–169.
S. S. Smale [1970b] "Topology and Mechanics, Part II," *Inventiones Mathematicae*, **11**, 45–64.
N. Tarnow and J. C. Simo [1992] "How To Make Your Favorite Second-Order Algorithm Fourth-Order," preprint.
E. T. Whittaker [1959] *A Treatise on the Dynamics of Particles and Rigid Bodies, with an Introduction to the Problem of Three Bodies*, Cambridge, 1904; 4th ed., 1937; Dover ed., 1959.
J. Wisdom and M. Holman [1991] "Symplectic Maps for the N-body Problem," *The Astronomical Journal*, **102** (4), 1528–1538.
J. Wisdom and M. Holman [1992] "Symplectic Maps for the N-body Problem: Stability Analysis," preprint, March 31, 1992.
G. Zhong and J. E. Marsden [1988] "Lie–Poisson Hamilton–Jacobi Theory and Lie–Poisson Integrators," *Physics Letters A*, **33:3**, 134–139.